Master's Thesis

Master's degree in Energy Engineering

Strategies for monitoring the hydrogen production in a PEM electrolyser

REPORT

July 3, 2023

Author: Jorge Moreno García-Moreno

Advisor: Roser Capdevila Paramio

Co-advisor: Elisabet Mas de les Valls Ortiz

Call: July 2023

ETSEIB

Escola Tècnica Superior
d'Enginyeria Industrial de Barcelona

UPC

Abstract

The growing interest in the use of hydrogen as an energy resource has led to the search for new ways to produce it. In order to alleviate and mitigate the greenhouse gases emissions caused by the use of fossil fuels, one of the methods of hydrogen production is through PEM electrolysers. Using electricity, which can come from renewable energy sources, water can be dissociated generating oxygen and hydrogen. However, this hydrogen production method still does not present competitive costs with respect to other methods that do generate greenhouse gases, such as natural gas reforming.

Within the scope of opening a new research line about electrolysers, this project lays the foundations for research from a thermodynamic point of view, which will continue in the future with more works. The PEM electrolyser used in this project corresponds to an academic demonstration experiment that has a single cell. The first variables necessary to monitor are the voltage and current applied to the electrolyser, to later monitor the operating temperature of the electrolyser and the hydrogen production.

During the experimental stage carried out in the laboratory, an Arduino microcontroller has been used to collect data digitally, since it allows a high sampling rate, except for the production of hydrogen, which has been carried out analogically. Finally, the current and voltage have been measured thanks to the INA219 module and the temperature through thermocouples and MAX31855 modules. To establish and maintain the operating temperature of the electrolyser constant, an external hydraulic circuit has been made, manufacturing a heat exchanger through which the heated water with impurities from a water bath circulates, heating the distilled water which with the electrolyser is fed.

One of the long-term objectives of the open research line is the thermodynamic monitoring of the reaction, trying to measure the temperature values inside the electrolyser and not only in the inlet or outlet tubes. This would allow studying the influence of the geometry of the water channels on the operation of the electrolyser. As the laboratory has a thermal imaging camera and the electrolyser used has a methacrylate casing, a test has been carried out but it has been possible to verify that the methacrylate used by the manufacturer is not transparent to the infrared radiation detected by the camera, being impossible to accurately measure the evolution of the temperature caused by the electrochemical reaction.

Finally, the polarization curves of the electrolyser at different operating temperatures have been obtained, being able to verify that the higher the inlet water temperature, the higher the voltage applied to the electrolyser is at the same current density. This difference is more accused when the current density is higher. A correlation has also been found between the polarization voltage of the electrolyser during its startup depending on the current rate applied, and moreover, once the electrolyser is turned off, it remains polarized for about 7 hours. However, the hydrogen monitoring method used has not been adequate since the Faraday efficiency obtained does not have a logical value.

ETSEIB

Resumen

En los últimos años el creciente interés en el uso de hidrógeno como recurso energético ha propiciado la búsqueda de nuevas formas para su producción. Con el fin de paliar y mitigar la emisión de gases de efecto invernadero por el uso de combustibles fósiles, uno de los métodos de producción de hidrógeno es mediante electrolizadores PEM. Usando electricidad, pudiendo provenir de fuentes de energía renovables, se puede disociar agua generando oxígeno e hidrógeno. Sin embargo, este método de producción de hidrógeno aún no presenta unos costes competitivos con respecto a otros métodos que si generan gases de efecto invernadero como puede ser el reformado de gas natural.

En el ámbito de la apertura de una nueva línea de investigación en los electrolizadores, este proyecto senta las bases para la investigación desde un punto termodinámico de los electrolizadores, que continuará con más trabajos futuros. El electrolizador PEM utilizado en este proyecto corresponde a un experimento de demostración académica que dispone de una única celda. Las primeras variables necesarias a monitorizar corresponden con el voltaje y la corriente aplicadas al electrolizador, para más tarde monitorizar la temperatura de operación del electrolizador y la producción de hidrógeno.

Durante la fase experimental realizada en el laboratorio se ha utilizado un microcontrolador arduino para la toma de datos de forma digital ya que esto permite tener una tasa de muestreo elevada, a excepción de la producción de hidrógeno que se ha realizado de forma analógica. Finalmente, la corriente y el voltaje han sido medidos gracias al módulo INA219 y la temperatura mediante termopares y módulos MAX31855. Para establecer y mantener constante la temperatura de operación del electrolizador, se ha realizado un circuito hidráulico externo, fabricando un intercambiador de calor por el que circula el agua con impurezas del baño térmico y que calienta el agua destilada de entrada al electrolizador.

Uno de los objetivos a largo plazo de la línea de investigación abierta es la monitorización termodinámica de la reacción, tratando de medir los valores de temperatura dentro del electrolizador y no sólo en los tubos de entrada o salida. Esto permitiría estudiar la influencia de la geometría de los canales de agua en la operación del electrolizador. Como en el laboratorio se dispone de una cámara térmica y el electrolizador utilizado dispone de un carcasa de metacrilato, se ha realizado una prueba pero se ha podido comprobar que el metacrilato utilizado por el fabricante no es transparente a la radiación infrarroja que detecta la cámara, siendo imposible medir de forma precisa la evolución de la temperatura causada por la reacción electroquímica.

Finalmente se han obtenido las curvas de polarización del electrolizador a diferentes temperaturas de operación, pudiendo comprobar que a mayor temperatura del agua de entrada, el voltaje aplicado al electrolizador a una misma densidad de corriente es superior. Siendo esta diferencia más notable cuando la densidad de corriente es mayor. También se ha encontrado correlación entre el voltaje de polarización del electrolizador durante su arranque en función de la velocidad con que se aplica la corriente, y que una vez se apaga el electrolizador, este permanece polarizado durante unas 7 horas. Sin embargo, el método de monitorización de hidrógeno utilizado no ha sido el correcto ya que la eficiencia de Faraday obtenida no tiene un resultado lógico.

ETSEIB

Resum

En els últims anys el creixent interès en l'ús d'hidrogen com a recurs energètic ha propiciat la cerca de noves formes per a la seva producció. Amb la finalitat de pal·liar i mitigar l'emissió de gasos d'efecte d'hivernacle per l'ús de combustibles fòssils, un dels mètodes de producció d'hidrogen és mitjançant electrolizadores PEM. Usant electricitat, podent provenir de fonts d'energia renovables, es pot dissociar aigua generant oxigen i hidrogen. No obstant això, aquest mètode de producció d'hidrogen encara no presenta uns costos competitius respecte a altres mètodes que si generen gasos d'efecte d'hivernacle com pot ser el reformat de gas natural.

En l'àmbit de l'obertura d'una nova línia de recerca en els electrolizadores, aquest projecte senta les bases per a la recerca des d'un punt termodinàmic dels electrolizadores, que continuarà amb més treballs futurs. El electrolizador PEM utilitzat en aquest projecte correspon a un experiment de demostració acadèmica que disposa d'una única cel·la. Les primeres variables necessàries a monitorar corresponen amb el voltatge i el corrent aplicades al electrolizador, per a més tard monitorar la temperatura d'operació del electrolizador i la producció d'hidrogen.

Durant la fase experimental realitzada en el laboratori s'ha utilitzat un microcontrolador arduino per a la presa de dades de manera digital ja que això permet tenir una taxa de mostreig elevada, a excepció de la producció d'hidrogen que s'ha realitzat de manera analògica. Finalment, el corrent i el voltatge han estat mesurats gràcies al mòdul INA219 i la temperatura mitjançant termoparells i mòduls MAX31855. Per a establir i mantenir constant la temperatura d'operació del electrolizador, s'ha realitzat un circuit hidràulic extern, fabricant un bescanviador de calor pel qual circula l'aigua amb impureses del bany tèrmic i que escalfa l'aigua destil·lada d'entrada al electrolizador.

Un dels objectius a llarg termini de la línia de recerca oberta és el monitoratge termodinàmic de la reacció, tractant de mesurar els valors de temperatura dins del electrolizador i no sols en els tubs d'entrada o sortida. Això permetria estudiar la influència de la geometria dels canals d'aigua en l'operació del electrolizador. Com en el laboratori es disposa d'una cambra tèrmica i el electrolizador utilitzat disposa d'un carcassa de metacrilat, s'ha realitzat una prova però s'ha pogut comprovar que el metacrilat utilitzat pel fabricant no és transparent a la radiació infraroja que detecta la càmera, sent impossible mesurar de manera precisa l'evolució de la temperatura causada per la reacció electroquímica.

Finalment s'han obtingut les corbes de polarització del electrolizador a diferents temperatures d'operació, podent comprovar que a major temperatura de l'aigua d'entrada, el voltatge aplicat al electrolizador a una mateixa densitat de corrent és superior. Sent aquesta diferència més notable quan la densitat de corrent és major. També s'ha trobat correlació entre el voltatge de polarització del electrolizador durant la seva arrencada en funció de la velocitat amb què s'aplica el corrent, i que una vegada s'apaga el electrolizador, aquest roman polaritzat durant unes 7 hores. No obstant això, el mètode de monitoratge d'hidrogen utilitzat no ha estat el correcte ja que l'eficiència de Faraday obtinguda no té un resultat lògic.

ETSEIB

Acknowledgements

To my parents, Bienve and Goyi, for all the support in difficult moments, for trusting me even when things went wrong and for providing me everything and much more.

I would like to express my gratitude to my two advisors, Roser and Eli, for their guidance and support throughout the project, and for all the solutions that without your help and speed we would not have achieved.

To my friends, those from my childhood in Toledo and the most recent ones from Barcelona. Without you nothing would have been the same, for all the calls, coffees, dinners and trips that have helped me to recharge the energy in difficult moments.

ETSEIB

Contents

ETSEIB

List of Figures

ETSEIB

List of Tables

Listings

ETSEIB

Preface

Project origin

The use of hydrogen-based technologies has gotten interest in recent years due to its great potential. In its fight against climate change, the European Union (EU) has shown great interest in hydrogen as a clean and sustainable energy source because it is considered a promising alternative to fossil fuels, as it can be produced from renewable sources avoiding carbon dioxide emissions.

The growing interest in these technologies opens research fields that today have not been completely explored, in order to improve existing technology. For this reason, the two advisors have decided to put their experience in thermodynamics in the opening of new lines of research in the hydrogen production.

Incentive

Currently there exists already hydrogen production systems using renewable sources available at an industrial level. However, the cost of the hydrogen produced is not low enough to compete against other less sustainable production methods. The most proliferated electrolysers are of the PEM type and although they have been extensively studied from an electrochemical point of view, they have not been deep studied from a thermodynamic point of view.

Therefore, the motivation of this work is to lay the foundations for laboratory experimentation about the monitoring of PEM electrolysers. As it is the beginning of a new line research, it is necessary to establish a correct electrical data collection system, so later continue with deeper thermodynamic studies.

Prerequisites

Due to the project characteristics, it is necessary to have some theoretical background about chemistry, electricity and electronics, thermodynamics and programming, among others. The big experimental weight of the work makes it crucial to have skills for manual work and problem solving. Thanks to studies in industrial engineering and renewable energy engineering, the author has the theoretical knowledge having studied subjects such as chemical engineering, advanced electronics, thermal machines, thermal machines extension and programming. Finally, the practical experience obtained by the author because of having at home a small workshop with manual machines, lathe, milling machine, etc, together with the participation in the formula student association, allow him to face the practical realization of this project.

ETSEIB

1 Introduction

1.1 Objectives

Throughout this work, the study of the water electrolysis for the generation of hydrogen and oxygen is pursued. Using a PEM electrolyser for academic demonstration, the objective is to monitor the most important variables of the electrolyser operation. These variables are both the current and the voltage of the electrolyser, as well as the existing temperatures in different parts of the assembly, the existing gradients, and the hydrogen production.

This experimental project is the beginning of a line of research, and it is important to lay a good foundation for future work. For this reason, another of the objectives is to collect the data digitally, allowing data to be acquired with a high read rate, accurately and automatically.

The monitoring should allow not only the electrical analysis of the water dissociation reaction, but also the thermal analysis at different operating temperatures.

Finally, the monitoring system must be flexible to be able to easily adapt to other electrolysers in order to allow both the monitoring of the electrolyser presented in this work and future PEM electrolysers with different characteristics that could be monitored in the future.

1.2 Scope

The scope of this work consists in the use of an academic demonstration PEM electrolyser to obtain its polarization curves and hydrogen production at different temperatures. It will be necessary to make changes to the electrolyser used, but all the changes made are considered not to be definitive, and for this reason they must all be reversible.

Finally, the operating limits to be used are those indicated by the manufacturer. This fact makes it possible to extend the useful life of the electrolyser, avoiding any malfunction , but it also limits the results to be obtained, having less extensive graphs.

ETSEIB

2   Literature review

2.1   State of art

One of the biggest concerns of governments, scientific community and people all around the world is the climate change. Climate change refers to the long-term changes in the Earth's climate, including changes in temperature, precipitation, and weather patterns, that have been observed over several decades or longer. It is primarily caused by human activities, particularly the emission of greenhouse gases such as carbon dioxide, methane, and nitrous oxide, which trap heat in the Earth's atmosphere and lead to a warming of the planet.

The effects of climate change are becoming increasingly evident and include rising sea levels, more frequent and severe heatwaves, droughts and floods, changes in the timing and intensity of precipitation, and more intense storms and hurricanes. These changes have significant impacts on human societies and ecosystems, including increased risk of wildfires, crop failures, and water scarcity, as well as the loss of biodiversity and the degradation of ecosystems.

Climate change is a complex and multifaceted problem, and its impacts are not evenly distributed across the globe. Some regions and communities are more vulnerable to its effects than others, particularly those in low-lying coastal areas or regions with limited resources and infrastructure to cope with extreme weather events [1].

Addressing climate change requires a coordinated global effort to reduce greenhouse gas emissions and adapt to the changing climate. It includes measures such as transitioning to low-carbon energy sources, improving energy efficiency, implementing sustainable land-use practices, and research and development of new technologies to mitigate the impacts of climate change. All this measures pursuit, in the end, the decarbonisation of the human activity [2].

Decarbonisation refers to the process of reducing and ultimately eliminating carbon dioxide and other greenhouse gas emissions from the atmosphere. The main sources of greenhouse gas emissions are energy production, transportation, industry, agriculture, and land use. The burning of fossil fuels such as coal, oil, and natural gas for energy production (electricity and heat) is the largest source of carbon dioxide emissions, accounting for around 31% of global emissions. Transportation is the second largest source, accounting for around 15% of total emissions, while industry (12%), agriculture (11%), and land use change contribute smaller but still significant amounts of emissions [3].

ETSEIB
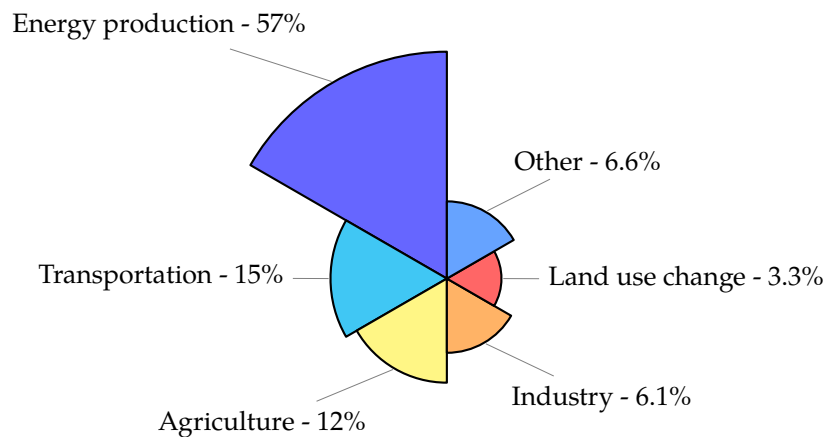
Figure 1: Primary sources of greenhouse emissions

There are several strategies and technologies that can be used to achieve decarbonisation. One approach is to increase energy efficiency, which reduces the amount of energy required to meet a given level of demand. This can be achieved through measures such as building insulation, energy-efficient appliances, and improved industrial processes.

Another approach is to shift to low-carbon energy sources, such as renewable energy and nuclear power. Renewable energy sources such as solar, wind, and hydropower do not emit greenhouse gases during operation and have become increasingly cost-competitive with fossil fuels in many parts of the world. Nuclear power also does not emit greenhouse gases during operation but must face challenges related to cost, safety, highly hazardous generation waste, and public acceptance.

Carbon capture, utilization and storage (CCUS) technologies can also be used to reduce emissions from fossil fuel use. CCUS involves capturing carbon dioxide emissions from industrial processes or power plants, and either storing them underground or using them for industrial applications such as enhanced oil recovery or the production of chemicals.

In addition, changes to land use and agricultural practices can also help to reduce emissions. For example, afforestation, which involves planting trees on land that was previously used for other purposes, can help to absorb carbon dioxide from the atmosphere. Changes to agricultural practices such as reducing tillage, improving soil management, and using more efficient fertilizers can also reduce emissions from agriculture.

Countries around the world have come together to negotiate and sign international agreements aimed at reducing greenhouse gas emissions and limiting the impacts of climate change. The most well-known of these agreements is the Paris Agreement, which was signed by 196 countries in 2015 and aims to limit global warming to well below 2 degrees Celsius above pre-industrial levels.

Under the Paris Agreement framework, governments are promoting the transition to renewable energy sources, such as wind, solar, and hydropower, which is a key strategy for reducing greenhouse gas emissions. Other action being taken is improving energy efficiency, involving measures such as building insulation, efficient lighting and appliances, and better transportation systems.

Efforts are being made to reduce emissions from cars, trucks, ships, and airplanes, leading to a more sustainable transportation. This can involve promoting public transportation, encouraging the use of electric and hybrid vehicles, and improving fuel efficiency. Moreover, many governments are implementing carbon pricing mechanisms, such as carbon taxes or cap-and-trade systems, to encourage businesses and consumers to reduce their greenhouse gas emissions.

Finally, planting trees and other vegetation is an effective way to remove carbon dioxide from the atmosphere and store it in biomass. Efforts are being made to reforest degraded lands, restore degraded ecosystems. However, and related to this topic, agriculture is another significant contributor to greenhouse gas emissions, particularly through deforestation, livestock production, and the use of synthetic fertilizers. Efforts are being made to promote sustainable agriculture practices, such as agroforestry, conservation agriculture, and organic farming, which can reduce greenhouse gas emissions and increase carbon sequestration in soils.

Governments around the world are increasingly recognizing the potential of hydrogen as a key component of their strategies to combat climate change. Hydrogen is a versatile and clean energy carrier that can be produced from a variety of sources, including renewable energy sources such as wind and solar power, and can be used to power a range of applications, including transportation, industry, and electricity generation.

Governments are looking to hydrogen as a way to decarbonise their energy systems, particularly in sectors such as transportation and industry. Hydrogen fuel cell vehicles, for example, emit only water vapor and have the potential to significantly reduce greenhouse gas emissions from the transportation sector. Hydrogen can also play a role in supporting the integration of renewable energy sources into the grid. Excess renewable energy can be used to produce hydrogen through electrolysis, and the hydrogen can then be stored and used to generate electricity when needed. This can help to balance the intermittent output of renewable energy sources and provide grid stability. Hydrogen can also be used as a feedstock in the production of chemicals, fertilizers, and other industrial products, and can be used to decarbonise industrial processes that are currently reliant on fossil fuels [4].

The main drawbacks of hydrogen nowadays are due to the immaturity of the technology, leading to low efficiencies and the need of use rare materials such as platinum; and the lack of a solid infrastructure. Governments and private companies are investing in the development of hydrogen technology and infrastructure, such as refueling stations for hydrogen fuel cell vehicles, pipelines for transportation, new ways to produce and store hydrogen, and alternatives to produce final work from the hydrogen stored due to the potential of the technology [5].

2.2   Hydrogen production methods

Hydrogen is a versatile and abundant element that has the potential to play a significant role in the transition to a low-carbon economy. Hydrogen is the lightest and most abundant element in the universe, making up about 75% of its elemental mass. On Earth, hydrogen is typically found in compounds such as water, hydrocarbons, and biomass.

ETSEIB

Hydrogen has several unique properties that make it a desirable energy carrier, including its high energy content per unit mass, low emissions when used as fuel, and its ability to be produced from a variety of renewable sources. The hydrogen can be produced from unlike sources by making use of different technologies. The main methods to produce hydrogen are:

2.2.1 Thermochemical Processes

$\longmapsto$ **Natural gas reforming:** also called steam methane reforming (SMR), is a process that uses high-temperature steam (700°C - 1000°C) to produce hydrogen from methane. Theoretically, in SMR the methane reacts with the steam in presence of a catalyst (mainly nickel and platinum group materials [7]) at a pressure of 3-25 bar, producing hydrogen and carbon oxides. The main reaction happening gives rise to carbon monoxide, whose stoichiometric reaction is shown in the equation 1.

$$CH_4 + H_2O \longrightarrow CO + 3H_2 \tag{1}$$
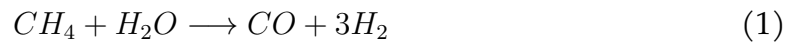
However, in practice a small amount of undesired carbon dioxide is also produced. The reaction is shown in equation 2.

$$CH_4 + 2H_2O \longrightarrow CO_2 + 4H_2 \tag{2}$$
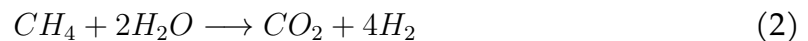
$\longmapsto$ **Partial oxidation:** during this process, methane and other hydrocarbons presented in natural gas react with limited oxygen, usually from the air. Since less oxygen than needed is available, the reaction products contain primarily hydrogen and carbon monoxide, and a relatively small amount amount of carbon dioxide or nitrogen compounds if the oxygen fueled is not pure and comes from the air. The stoichiometric reaction is as follows in equation 3.

$$CH_4 + \frac{1}{2}O_2 \longrightarrow CO + 2H_2 \tag{3}$$
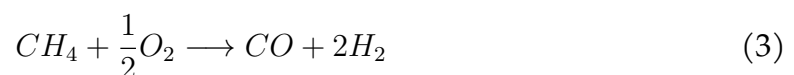
$\longmapsto$ **Biomass gasification:** with a controlled amount of oxygen and /or steam, organic material is converted into carbon monoxide, carbon dioxide, hydrogen and other species. The reaction takes place at more than 700°C without combustion and all the resultant species are in gas state, for that reason adsorbers or membranes are needed to separate the hydrogen from the resultant gas stream. The organic materials used can present different and complex compositions; depending on that, other species can be obtained in the reaction. The equation 4 shows the stoichimetric reaction when glucose is used.

$$C_6H_{12}O_6 + O_2 + H_2O \longrightarrow CO + CO_2 + 2H_2 + other\ species \tag{4}$$
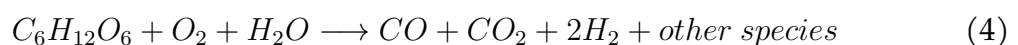
One of the resultant species of the three aforementioned processes, the CO, has a global warning potential (GWP) around 2.8 meaning that having the same amount of CO_2 and

CO, the CO will contribute 2.8 more to the global warming. Moreover, CO is an odorless, colorless and tasteless gas that can kill a person if it is inhaled. 80,000 ppm (parts per million) of CO_2 are considered to be life threatening while just 1,500 ppm of CO are considered for the same consequences [8]. For these reasons, it is preferable to produce CO_2 rather than CO. The use of the named **water-gas shift reaction** besides the presented methods, allow not only to convert the CO into CO_2, but to produce more hydrogen using the same amount of fuels. In the water-gas shift reaction the combination of carbon monoxide and steam in presence of a catalyst produce carbon dioxide and hydrogen, as the equation 5 shows [6].

$$CO + H_2O \longrightarrow CO_2 + H_2 \tag{5}$$

$\longmapsto$ **Solar thermochemical water splitting:** this process consumes water to produce hydrogen and oxygen, however it is needed high temperature heat (up to 2,000°C) and some chemicals that are not consumed and can be reused within each cycle. There exists numerous thermochemical water-splitting cycles, where each have different conditions and chemicals used. Usually, the high temperature heat is produced by a reactor tower using a field of heliostat, a parabolic dish concentrator or using waste from nuclear reactors.

As an example, it is presented the cerium oxide two step cycle. Firstly, the cerium (IV) oxide is heated up to 2,000°C producing cerium (III) oxide and oxygen as the reduction equation 6 shows.

$$2Ce(IV)O_2 \longrightarrow Ce(III)_2O_3 + \frac{1}{2}O_2 \tag{6}$$
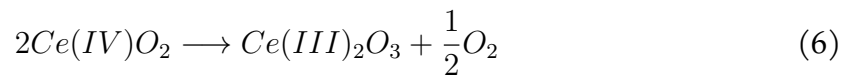
Finally, the cerium (III) oxide is combined with water at 400°C to produce cerium (IV) oxide and hydrogen gas. The oxidation equation is as follows in equation 7.

$$Ce(III)_2O_3 + H_2O \longrightarrow 2Ce(IV)O_2 + H_2 \tag{7}$$
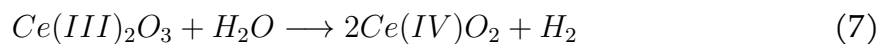
The net reaction of the cycle in equation 8 presents the production of oxygen and hydrogen using water as fuel.

$$Ce(III)_2O_3 + H_2O \longrightarrow 2Ce(IV)O_2 + H_2 \tag{8}$$
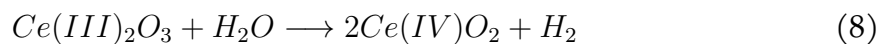
2.2.2 Biological processes

$\longmapsto$ **Microbial biomass conversion:** in this process microorganisms like bacteria, break down organic matter producing hydrogen. These are considered fermentation based systems, and the organic matter can be raw biomass, corn stover, wastewater or refined sugar among others. No light is required and so, it is also called "dark fermentation".

ETSEIB

⟶ **Photobiological:** the microorganisms present in this process are green microalgae and cyanobacteria, which use sunlight to split water into oxygen and hydrogen.

However, these two hydrogen production methods are in first stage of research and their main drawbacks are the low rates of hydrogen produced and the difficulty to maintain the production for long periods of time [6].

2.2.3 Electrolysers

Electrolysis is the process of using electricity to split water into hydrogen and oxygen. Electrolysers consist of an anode and a cathode separated by an electrolyte and each electrolyte function in a different way depending on their characteristics, the three main electrolysers will be described nextly.

⟶ **Alkaline:** in this typology of electrolyser two metallic electrodes are immersed in a liquid electrolyte. Aqueous solutions of KOH or NaHO are usually used in order to provide the fuel, water, conductivity characteristics. Usual concentration of electrolyte is around 40wt% to provide maximum electrical conductivity at temperatures up to 90°C, being enough because alkaline cells usualy operate at temperatures around 20°C to 80°C. Water reduction is produced at the cathode (electrode with negative potential), according to the equation 9, producing hydrogen and hydroxyl ions [10].[11]

$$2H_2O + 2e^- \longrightarrow H_2 + 2OH^- \tag{9}$$

Hydroxyl ions are oxidized at the cathode producing oxygen and water, as the equation 10 shows.

$$2OH^- \longrightarrow \frac{1}{2}O_2 + H_2O + 2e^- \tag{10}$$
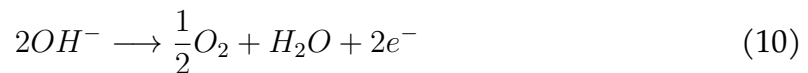
Adding equations 9 and 10, the net reaction equation 11 is obtained, which describes that pure hydrogen and oxygen can be obtained from water.

$$H_2O \longrightarrow H_2 + \frac{1}{2}O_2 \tag{11}$$

For the operation of the alkaline electrolyser only water is consumed, apart from electricity, being needed to continuously feed the cell in order to maintain the electrolyte concentration constant. Moreover, if hydrogen and oxygen are in contact, they will react spontaneously producing water. For that reason, there exist a cell separator through which the hydroxyl ions can cross while hydrogen and oxygen are kept in each side of the separator. In figure 2 a schematic of the alkaline electrolyser is shown.

ETSEIB
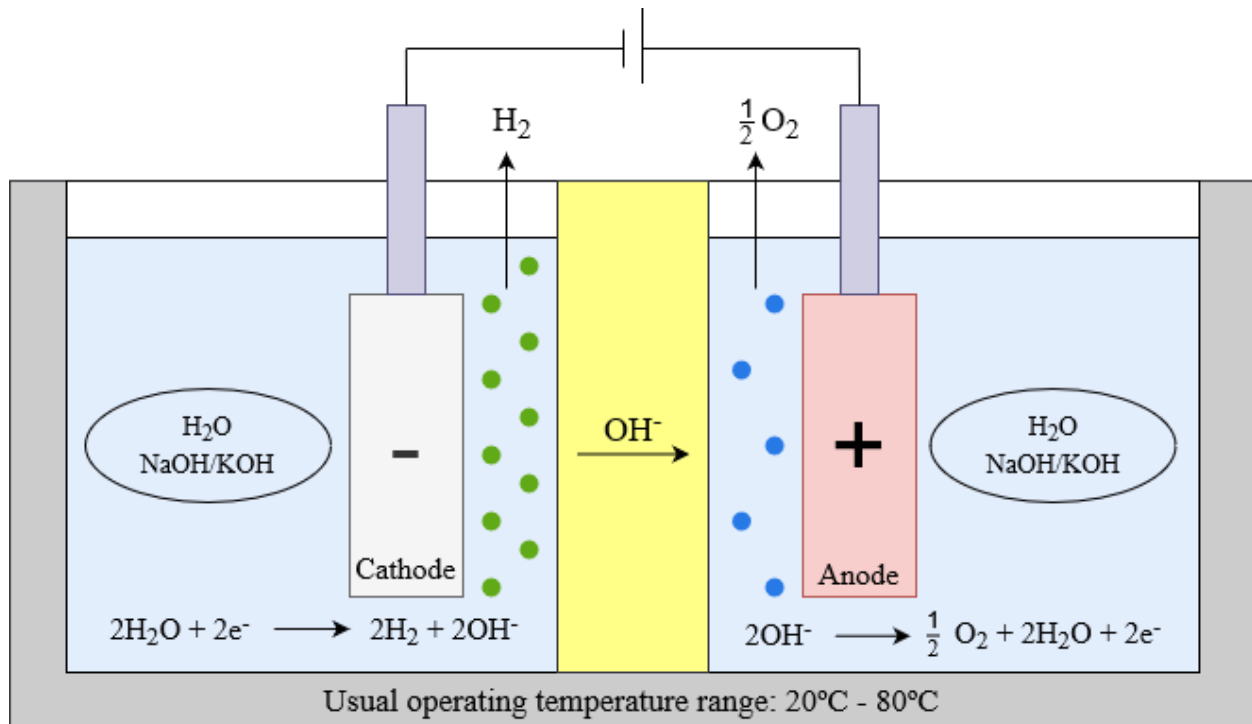
Figure 2: Alkaline electrolysis cell diagram

$\longmapsto$ **PEM:** in the proton exchange membrane (PEM) electrolyser the two electrodes are in contact with the the proton conducting polymer electrolyte, forming a so-called membrane electrode assembly (MEA). The fuel in which the MEA is immersed in pure water and the reaction taking place at the anode is the production of oxygen and hydrogen ions consuming water, as the equation 12 presents. As well as alkaline cells, PEM cells usually operate at temperatures around 20°C to 80°C and so, liquid water is used.

$$H_2O \longrightarrow \frac{1}{2}O_2 + 2H^+ + 2e^- \tag{12}$$
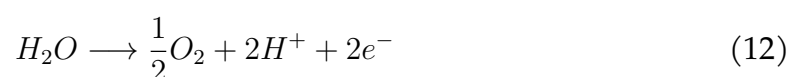
The hydrogen ions cross the MEA and the hydrogen is produced at the cathode.

$$H^+ + 2e^- \longrightarrow H_2 \tag{13}$$

Leading to an overall equation equal to the one presented for the alkaline electrolysis cell, although the species crossing from anode to cathode are different.

$$H_2O \longrightarrow H_2 + \frac{1}{2}O_2 \tag{14}$$

The schematic of a PEM electrolysis cell, including the partial reactions taking place at anode and cathode, can be seen in figure 3.
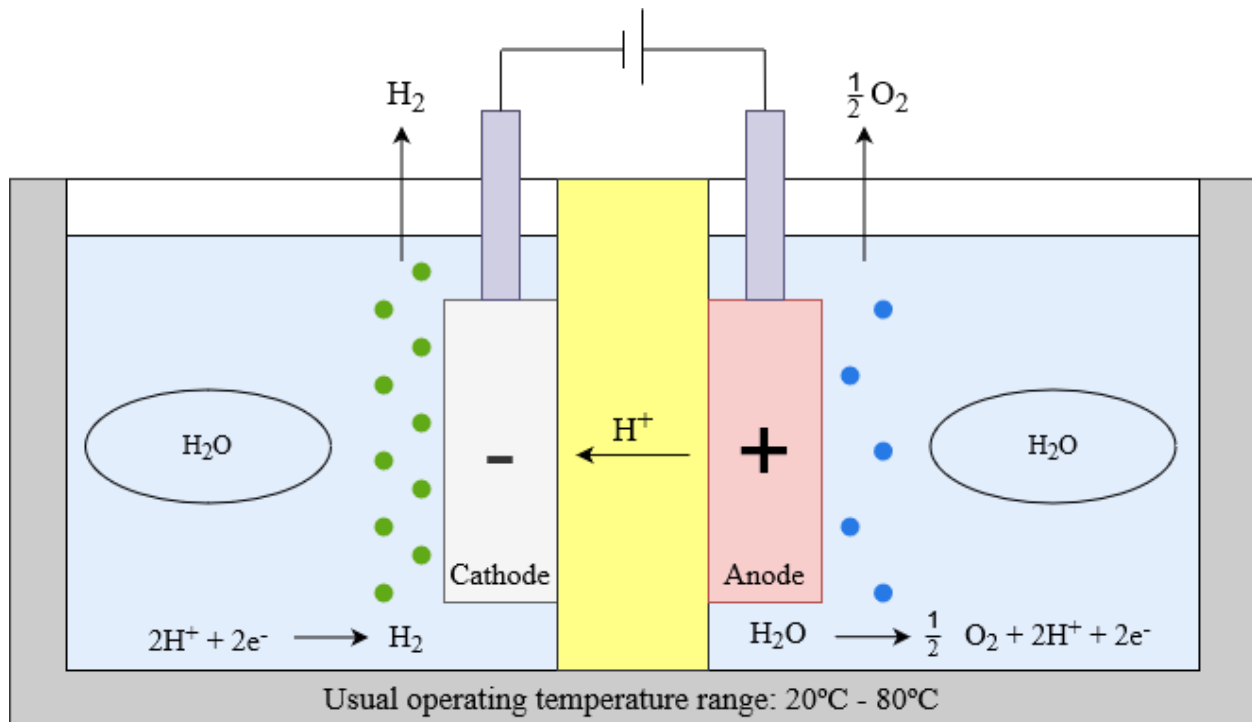
Figure 3: PEM electrolysis cell diagram

$\longmapsto$ **SOC:** the particularity of solid oxide cells (SOC) is the use of a oxide ion conducting ceramic materials as a solid electrolyte and cell separator (usually zirconia stabilized with yttrium and scandium oxides). These kind of cells usually operate at temperatures around 800°C-1,000°C and the water is in gas state. The water molecules are reduced in the cathode being split in hydrogen and oxygen ions according to equation 15.

$$H_2O + 2e^- \longrightarrow H_2 + O^{2-} \tag{15}$$

The oxygen ions cross the solid ceramic electrolyte to the anode, where the oxygen is produced.

$$O^{2-} \longrightarrow O_2 + 2e^- \tag{16}$$
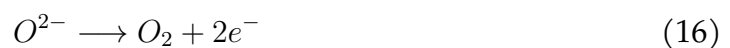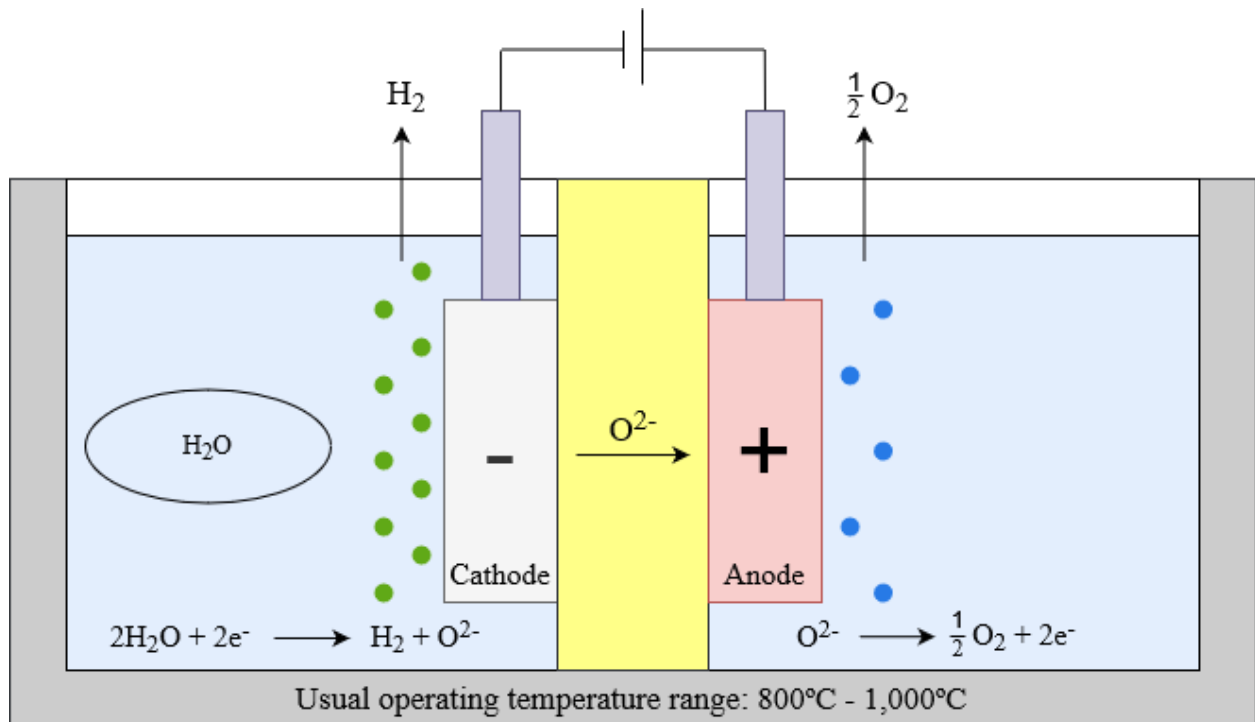
Figure 4: SOC electrolysis diagram

2.3   PEM electrolyser

Although the main electrochemical reactions that occur in an electrolyser are the ones already presented in equations 12, 13 and 14, some other phenomena take place simultaneously during the reaction. In the article [13] several physical principles presented in many other articles have been pieced together in order to provide a complete model of a PEM electrolyser. Moreover, the presented model was validated with experimental work in order to check its accuracy at different temperatures.

The model is composed of four subsections referring to anode and cathode chambers, the membrane and the voltage. It is also considered to be in steady-state conditions justified by the fact of the fast response of the PEM electrolysers. The molar balance happening in a PEM electrolyser during its operation is shown in figure 5, from which the rest of the model will be explained.

ETSEIB
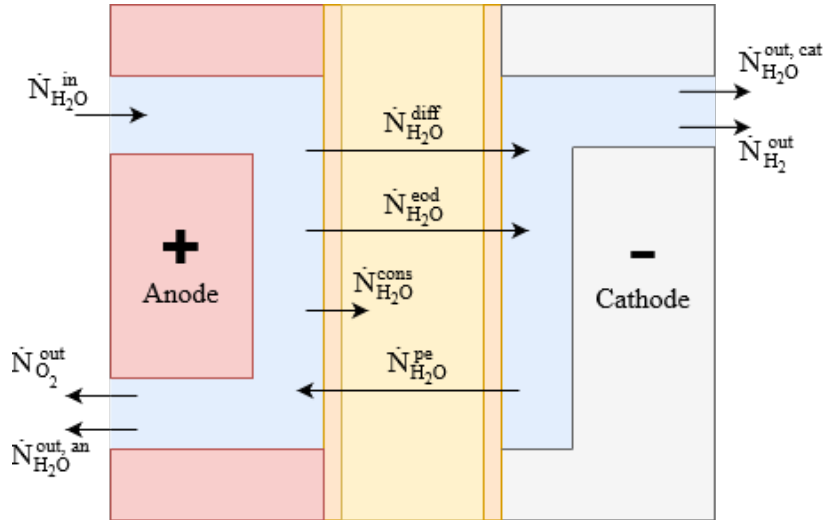
Figure 5: PEM electrolyser schematic

↦ **Anode chamber:** according to Faraday's law, four moles of oxygen are generated for each electron, and so two moles of water are consumed for each electron. The reaction takes place at the surface of the membrane, where the catalyst is placed. The equations showing this behaviour are described in 17 and 18, where F refers to the Faraday's constant with a value of 96.435 [C/mol].

$$\dot{N}_{O_2}^{gen} = \frac{1}{4F} \ [mol/s] \tag{17}$$

$$\dot{N}_{H_2O}^{cons} = \frac{1}{2F} \ [mol/s] \tag{18}$$

Ideally, the oxygen generated is the same as the output oxygen. However, if it is not the case, some oxygen will be accumulated, being expressed by the following equation 19 where the assumption that no oxygen is being carried by the water inlet flow is made.

$$\frac{d\dot{N}_{O_2}^{acc, \, an}}{dt} = \dot{N}_{O_2}^{gen} - \dot{N}_{O_2}^{out} \ [mol/s] \tag{19}$$

The accumulation of water in the anode chamber $\dot{N}_{H_2O}^{acc, \, an}$ can be calculated taking into account the water consumed during the reaction and the net water flow through the membrane $\dot{N}_{H_2O}^{mem}$ that will be explained later in this section. The equation 20 determines the water accumulation in the anode chamber.

$$\frac{d\dot{N}_{H_2O}^{acc, \, an}}{dt} = \dot{N}_{H_2O}^{in} - \dot{N}_{H_2O}^{cons} - \dot{N}_{H_2O}^{mem} - \dot{N}_{H_2O}^{out, \, an} \ [mol/s] \tag{20}$$

↦ **Cathode chamber:** the hydrogen produced in the cathode side is calculated equally as in the anode chamber, by the Faraday's law as it is set in the equation 21.

$$\dot{N}_{H_2}^{gen} = \frac{1}{2F} \ [mol/s] \tag{21}$$

The accumulation of hydrogen in the cathode chamber is also, and again, calculated making the difference between the hydrogen generated and extracted, as the equation 22 shows.

$$\frac{d\dot{N}_{H_2}^{acc, \ cat}}{dt} = \dot{N}_{H_2}^{gen} - \dot{N}_{H_2}^{out} \ [mol/s] \tag{22}$$

Finally, the water accumulated in the cathode chamber is caused by the difference between the water extracted and the water permeated through the membrane.

$$\frac{d\dot{N}_{H_2O}^{acc, \ cat}}{dt} = \dot{N}_{H_2O}^{mem} - \dot{N}_{H_2O}^{out, \ cat} \ [mol/s] \tag{23}$$

$\mapsto$ **Membrane:** the water transport across the membrane is caused by three main phenomena: diffusion, electro-osmotic drag and hydraulic pressure. Leading the sum of the water transport caused by each phenomena to the net water transport through the membrane.

$$\dot{N}_{H_2O}^{mem} = \dot{N}_{H_2O}^{diff} + \dot{N}_{H_2O}^{eod} - \dot{N}_{H_2O}^{pe} \ [mol/s] \tag{24}$$

Diffusion of water refers to its transport from lower to higher concentrations regions, prevalently from anode to cathode. The Fick's law is used to describe the diffusion behaviour, and assuming a linear gradient the resolution of the Fick's law is shown in equation 25, where A is the surface area of the membrane, D_w refers to the membrane water diffusion coefficient, δ_{mem} corresponds to the membrane thickness and $C_{H_2O}^{mem/cat}$ and $C_{H_2O}^{mem/an}$ are the water concentrations at the electrolyte/electrode interfaces.

$$\dot{N}_{H_2O}^{diff} = \frac{A \ D_w}{\delta_{mem}}(C_{H_2O}^{mem/cat} - C_{H_2O}^{mem/an}) \ [mol/s] \tag{25}$$

The water concentrations can be calculated by different empiric approaches, but in order to not extend the present document excessively, the reader is directed the source article [13] for further details.

The **electro-osmotic drag** represents the number of water molecules that are dragged by each mole of hydrogen protons throught the membrane. The equation 26 shows the influence of the osmotic drag coefficient n_d related with the hydrogen ions I/F

$$\dot{N}_{H_2O}^{eod} = \frac{n_d \ I}{F} \ [mol/L] \tag{26}$$

ETSEIB

The value of the osmotic drag coefficient n_d has been empirically calculated in other studies, however some studies determine an integer value, others observe correlation with temperature, and even with temperature and pressure. Moreover, the humidity of the membrane have an important impact on the osmotic drag coefficient. Due to the variability of the different studies, it has been determined to not include a specific way of calculating the osmotic drag in this theoretical framework.

The water transport due to **hydraulic pressure** is caused by the pressure differences between anode and cathode chambers Δp. The water density ρ_{H_2O}, viscosity μ_{H_2O} and molar mass M_{H_2O} influence the water transport due to the hydraulic pressure, as well as the membrane permeability to water K_{Darcy}, surface area and membrane thickness.

$$\dot{N}_{H_2O}^{pe} = K_{Darcy} \frac{A \, \rho_{H_2O} \, \Delta p}{\delta_{mem} \, \mu_{H_2O} \, M_{H_2O}} \ \ [mol/s] \tag{27}$$

$\mapsto$ **Voltage:** the voltage needed to produce hydrogen is composed of the cell potential at open circuit and three more overpotentials: activation, omhic and concentration; that will be explained down below.

$$V^{cell} = V_{oc} + V_{act} + V_{ohm} + V_{con} \ \ [V] \tag{28}$$

The **open circuit voltage** is described by the Nerst equation, although if it is rewritten in terms of partial pressures, it will be of the form shown in equation 29.

$$V_{oc} = E^0 + \frac{R \, T}{z \, F} \ \ln \left(\frac{p_{H_2}}{p_{cat}} \sqrt{\frac{p_{O_2}}{p_{an}}} \right) \ \ [V] \tag{29}$$

Where E^0 is the reversible cell voltage, which is dependent of the species involved in the reaction and can be calculated as follows in equation 30. Where ΔG_R^0 is the change in the Gibb's free energy at standard temperature and pressure (STP) and z is the number of electrons involved in the reaction.

$$E_0 = \frac{\Delta G_R^0}{z \, F} \ \ [V] \tag{30}$$

The **activation overpotential** represents the required overpotential, above the equilibrium potential, to overcome the activation barriers to transfer the electrons from the electrolyte to the electrode. It can be deducted from the Butler-Volmer equation, and it is explicit as follows in equation 31 where α is the charge coefficient, i is the current flowing and i_0 is the exchange current density.

$$V_{act} = \frac{R \, T}{\alpha \, F} \ arcsinh \left(\frac{i}{i_0} \right) \ \ [V] \tag{31}$$

The exchange current density i_0 depends on the physical properties of the membrane and catalyst material, such as temperature, radious of the catalyst molecules, roughness, fraction of the catalyst surface in contact with the membrane, etc.

The **ohmic overpotenical** is caused by the ionic loss predominant in the membrane, being dependent of the current i and membrane thickness δ_{mem} and conductivity σ_{mem}, as the equation 32 shows.

$$V_{ohm} = \frac{\delta_{mem}}{\sigma_{mem}} \, i \; [V] \tag{32}$$

Finally, the **concentration overpotential** takes into account the difference in charge carriers concentrations between the electrolyte and the electrodes surfaces, whose value can be obtained from the equation 33 where the concentrations of oxygen and hydrogen are involved at normal operation and at standard conditions.

$$V_{con} = \frac{R\,T}{4\,F} \, \ln\left(\frac{C_{O_2}^{mem/an}}{C_{O_2,\,0}^{mem/an}}\right) + \frac{R\,T}{2\,F} \, \ln\left(\frac{C_{H_2}^{mem/cat}}{C_{H_2,\,0}^{mem/cat}}\right) \; [V] \tag{33}$$

The results obtained in the study shows a good fit between the model prediction and the experimental data as it can be observed in figure 6. To plot the figure in this document with enough resolution, the data from the original graph have been extracted making use of the software tool WebPlotDigitizer, which uses image recognition in order to extract the different information from a graph.
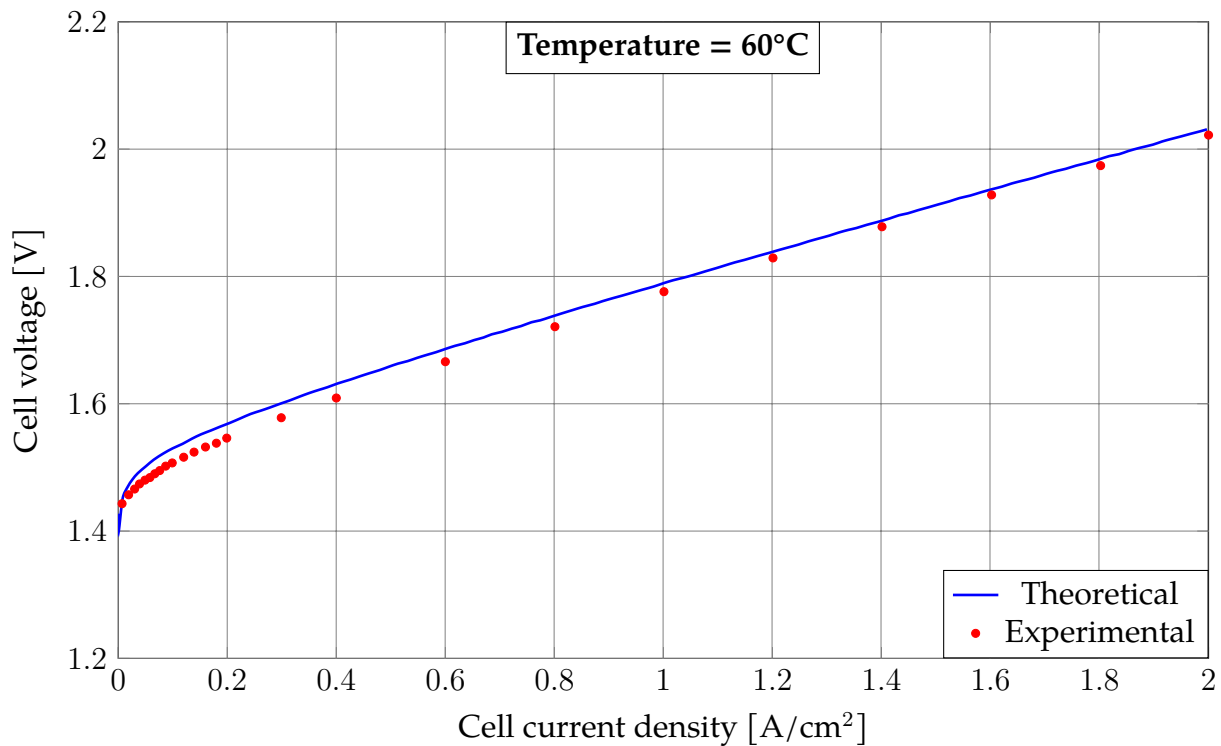

Figure 6: Model prediction and experimental data of PEM electrolyser at 60°C

3   Experimental methodology

During this section, the electrolyser that has been used will be presented, as well as its components and hydraulic and electrical circuits.

In order to characterize and deep understand the behaviour of the electrolyser it is necessary to monitor the variables of interest, taking into consideration the physical and practical limitations of the electrolyser available.

The main variables are, obviously, the current and voltage applied to the electrolyser, although some other variables considered are the temperatures existing in different points of the assembly.

The voltage and current data can be collected by using usual laboratory equipment such as multimeters in which the data measured should be read, and written or typed at the same instant of the reading. However, it is expected to perform several experiments with many measurements to be done, for that reason it has been decided to take all the measurements digitally through microprocessors which let taking the data readings faster while storing them.

The electrolyser assembly under study is composed by several components like the electrolyser cell itself, the input distilled water accumulator in which the oxygen produced is also evacuated, the hydrogen accumulator which is also filled with water in order to keep the cell pressure constant, and the different pipes that connect the accumulators with the cell. When the electrolyser is working not all the components will be at the same temperature, existing different gradients caused by thermal conduction and convection mainly.

The previous explanation must be taken into account when measuring the temperature of the electrolyser and for that reason, it has been decided to measure the temperature in two different ways. The first approach is by using thermocouples, providing the temperature measurement of the specific point in which each thermocouple is installed. The second method used to measure the temperature is using a thermal camera, which by measuring the infrared radiation emitted by the objects, its temperature map is captured in a picture.

Initially, there were available in the laboratory three microcontrollers to which different sensors could be connected, or even some data readings could be done directly with them. The three microcontrollers are: Odroid XU4 , Raspberry Pi 3b+ and Arduino 101. Although each one of them has specific features, the ones that have been a differentiating factor when choosing the microcontroller to use have been three.

The first one is the independence, since the Odroid and the Raspberry require the installation of an operating system, and they can work independently. However, the Arduino 101 does not have an operating system, requiring the programming of a script externally that is later installed on the board. This causes that for the Arduino a computer is necessarily needed from which to develop the necessary programming constantly, while in the Raspberry and the Odroid everything needed could be programmed directly.

The second feature is how spread they are. Both the Arduino and the Raspberry are widely used microcontrollers, for which there are numerous resources on the internet from which

ETSEIB

to obtain information. But the Odroid is not used that much, so any setback during the r4realisation of this work would require more time to solve it.

The third characteristic that was taken into account is the available communications on the board. Both the Odroid and the Arduino 101 have both digital and analog pinouts. However, the Raspberry only has digital communication pins.

Although a constant connection with a computer is necessary for coding the scripts, the great availability of resources together with the possibility of data reading through its analog pins (used in the first instance to measure voltages as will be seen below in the document) have been the reasons for selecting the Arduino 101 as the microcontroller to use [14] [15] [16].

3.1   Demonstration experiment

The electrolyser to be characterized and used in this project to monitor different variables of interest is included in the academic demonstration experiment shown in figure 7. In this experiment, from right to left, there is a small photovoltaic panel, the inlet water accumulator, the electrolyser, the outlet hydrogen accumulator, a fuel cell, and an electric motor that has a propeller coupled to its shaft. The objective of this demonstration experiment is to use solar energy to generate electricity thanks to the photovoltaic panel, this electricity is supplied to the electrolyser to produce hydrogen; and next the hydrogen is combined with atmospheric oxygen in the fuel cell to produce electricity and power the electric motor and the propeller. In the end, the solar energy is powering the electric motor using a lower efficiency, but demonstrating the feasibility of the hydrogen production and recombination.
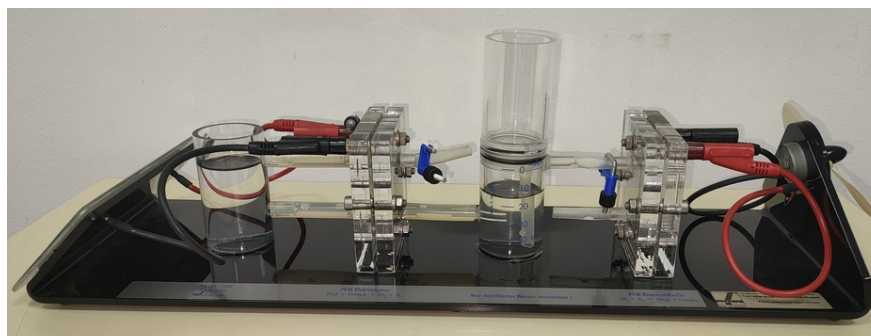
(a) Side view
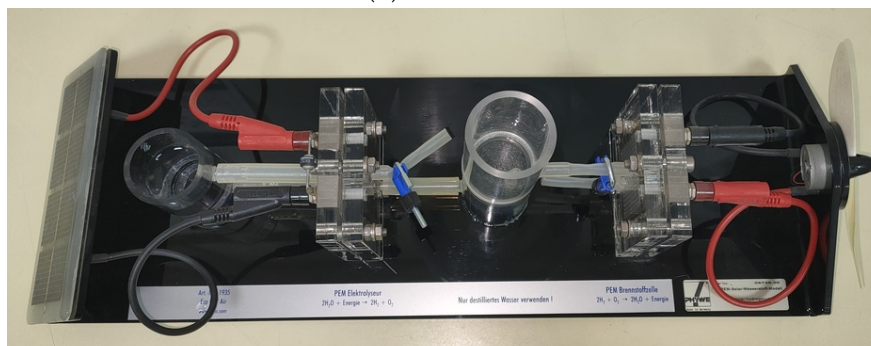
(b) Top view

Figure 7: Demo experiment

The demonstration experiment corresponds to an old and already discontinued model from Phywe company [17], which uses solar energy and distilled water to work. When carrying out the start-up of the experiment, it was verified that it was not working because the photovoltaic panel was not able of supplying the minimum voltage (1.5V according to the manufacturer's data sheet) to make the electrolyser to generate hydrogen. By supplying the necessary voltage and current through an external power supply, the experiment could be made to work. However, since the objective of the project is the electrolyser monitoring, from now on the focus will be in the electrolyser itself, and the two water and hydrogen accumulators. Excluding the interest in the photovoltaic panels, the fuel cell and the electric motor.

To explain in detail the operation of the electrolyser, the figure 8 is presented, which shows the hydraulic diagram of the demonstration experiment. The electrolyser can be observed, which has two outputs and one input. The input corresponds to distilled liquid water being fed from the accumulator in the left of the figure. The water is pushed towards the electrolyser due to its own hydrostatic pressure. As explained in the 2.3 section, the water dissociates into oxygen and hydrogen according to equation 14, and the gaseous oxygen generated together with the residual liquid water that has not reacted, leaves the electrolyser and returns to the liquid water accumulator. When gaseous oxygen returns to the accumulator, the oxygen is released to the environment since the accumulator is top open and having no additional accumulation method.

The hydrogen gas generated by the electrolyser is transported through its outlet pipe to the hydrogen accumulator. The hydrogen accumulator is made up of two tanks, upper and lower, which are connected by another pipe. The lower tank also has an outlet for hydrogen in its upper part. This outlet is the one that communicates with the fuel cell in case it is kept opened, and if it is kept closed it allows hydrogen to accumulate. The fact that both tanks are connected in the way shown in the diagram is important to allow the accumulation of hydrogen in the lower tank while avoiding a pressure increase. Before starting to generate hydrogen, the lower tank must be completely filled with water while the upper tank is empty. When producing hydrogen, the lower tank begins to fill with hydrogen bubbles, increasing its pressure and moving the water from the lower tank to the upper tank through the connection pipe.

ETSEIB
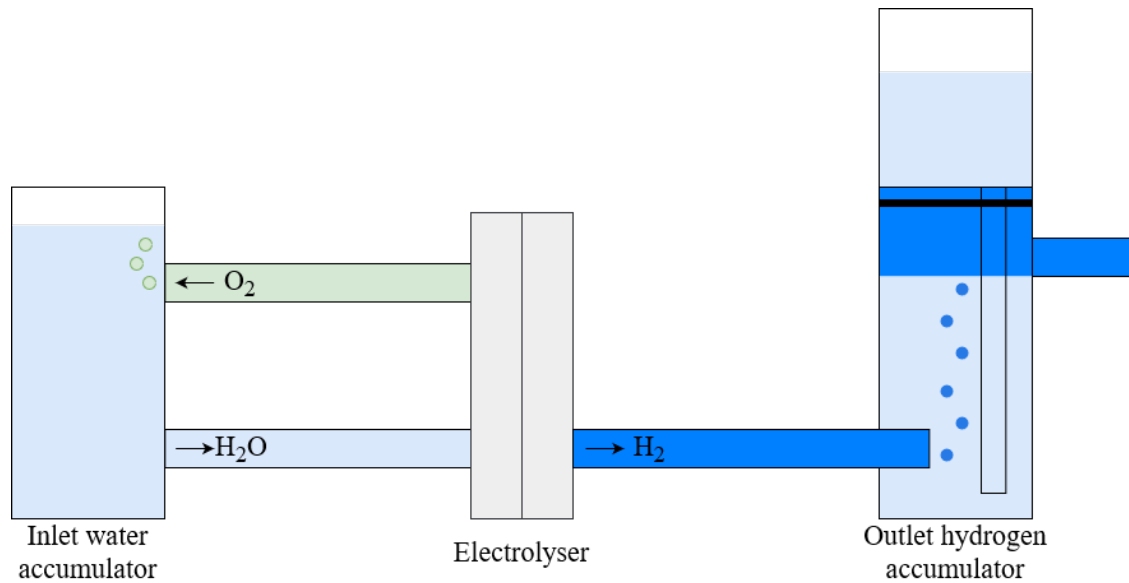
Figure 8: Electrolyser hydraulic scheme

The electrolyser itself has electrical inputs for the two terminals that feed it with direct current as shown in the figure 9. Each of the terminals is connected to two grillages that acts as the anode or cathode, and in between the MEA is placed, where the water dissociation reaction occurs. To maintain the entire electrolyser assembly, there exist two methacrylate plates fastened by screws and a sealant to prevent possible water, hydrogen or oxygen leaks.
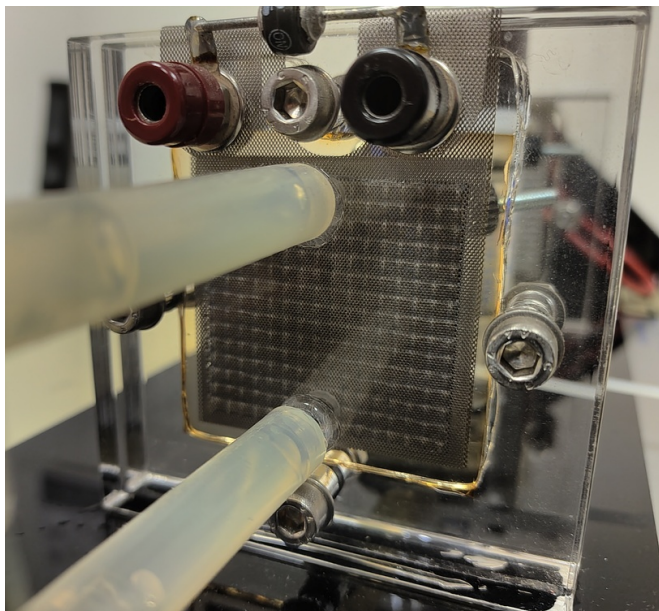
(a) Front view
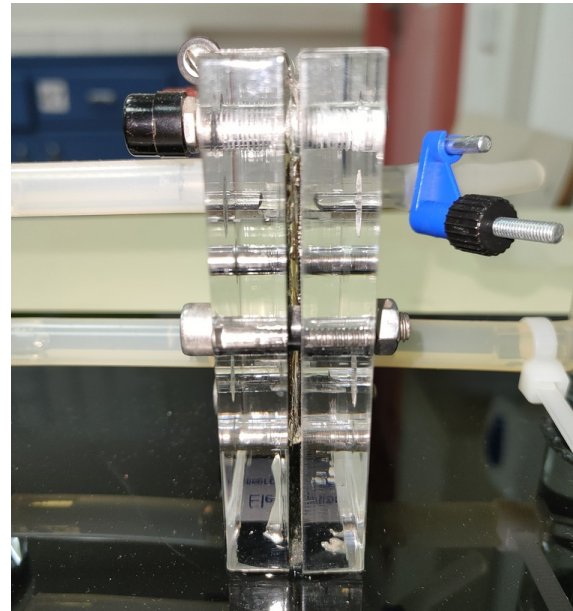
(b) Side view

Figure 9: Demonstration experiment electrolyser

The operation upper limits set by the manufacturer correspond to 2 [V] and 1.5 [A]. When the electrolyser is powered, there is no hydrogen generation before reaching input values

around 1.5 [V] and 0.6 [A]. This is caused due to the overpotentials needed to be overcome for the electrochemical reaction to occur, which has already been explained in section 2.3. When the reaction begins, small bubbles can be observed inside the electrolyser due to the fact that the methacrylate plates are translucent. In the figure 10a can observed the electrolyser when it is working and how the bubbles are formed in comparison with the figure 10b.

(a) Electrolyser working

(b) Electrolyser not working
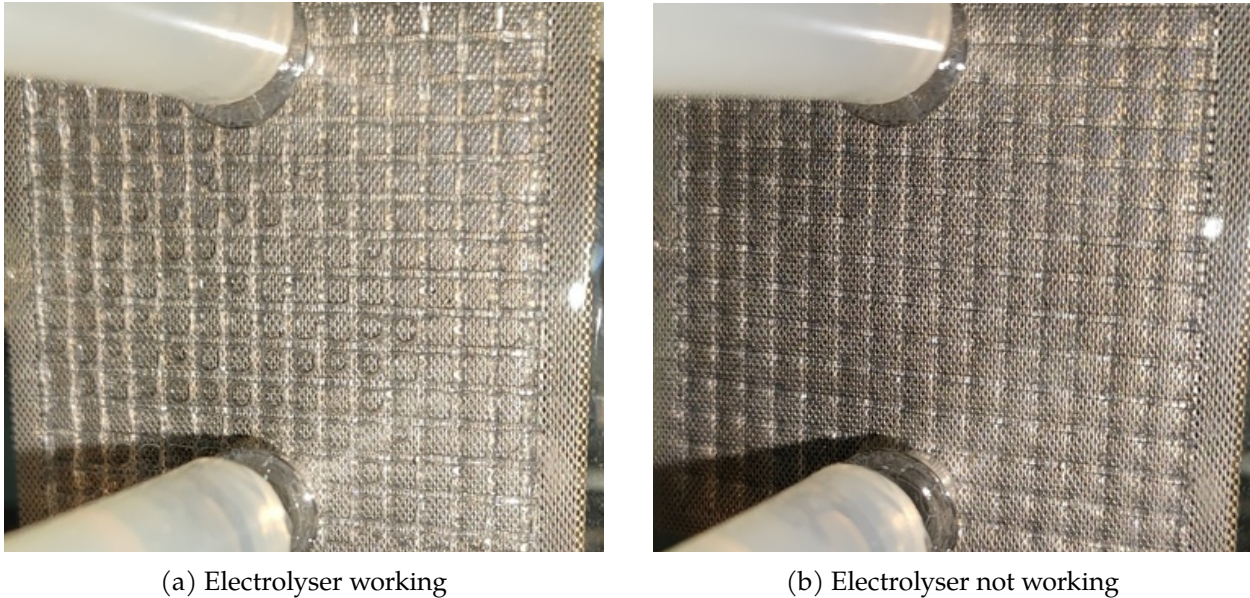
Figure 10: Demonstration electrolyser bubbles generation comparison in the grillage

3.2   Voltage and current

The first approach followed to measure the voltage across the two terminals of the cell, that is to say the voltage applied with the power supply, was just connecting two analog pins to the cell's terminals and subtracting their value. This way is suitable because the maximum possible reading is up to 5 [V] and the maximum admissible voltage to supply the cell, defined by the manufacturer is 2 [V].

The voltage measure is an analog signal although the value needed must be a decimal number. For that reason, the Arduino 101 is provided with a 8 bits analog-to-digital converter (ADC), being able to measure the voltage with a resolution of about 0.005 [V].

In order to measure the current exchanged between the power supply and the electrolyser making use of the Arduino 101 analog pins, it is needed to include a resistor in series. Knowing the value of the resistor and measuring the voltage drop across the resistor, the Ohm's law can be applied and the current flowing through the resistor is calculated, which is the same as the current flowing through the electrolyser.

The wiring diagram needed for the configuration is shown in figure 11, where the Arduino 101 is connected to the computer not only for powering it but also for setting the configuration and data visualization, using its own serial connection by USB port.

ETSEIB
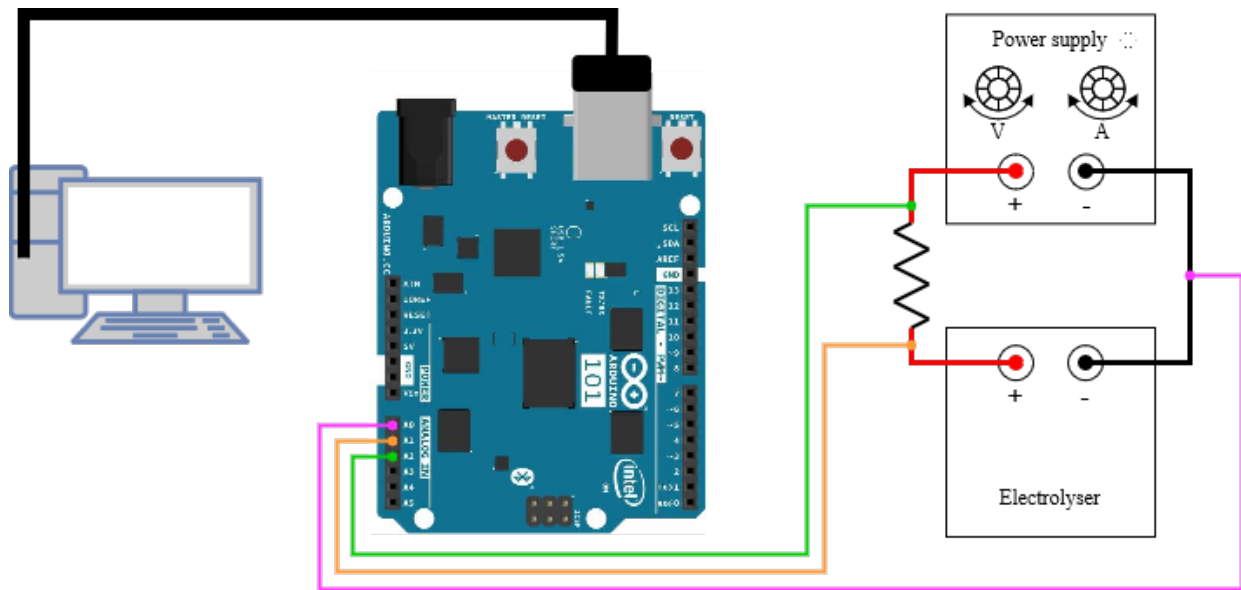
Figure 11: Wiring schematic for voltages readings with Arduino 101

Once the wiring is set, in order to make voltage readings of three voltages, no additional library is needed and the programmed code is the one shown in the code listing 1. Where the communication through the serial port is set at 9600 bits per second, which is a standard value. In the loop function, the sensor values are read using the "analogRead" function, providing a value between 0 and 1023; for that reason the integer number is then converted into a voltage value, and finally the voltage measurement is printed in the monitor.

```
1  void setup() {
2    Serial.begin(9600);
3  }
4  void loop() {
5    int sensorValue_A0 = analogRead(A0);
6    int sensorValue_A1 = analogRead(A1);
7    int sensorValue_A2 = analogRead(A3);
8    float voltage_pin0 = sensorValue_A0 * (5.0 / 1023.0);
9    float voltage_pin1 = sensorValue_A1 * (5.0 / 1023.0);
10   float voltage_pin2 = sensorValue_A3 * (5.0 / 1023.0);
11   Serial.println(voltage_pin0);
12   Serial.println(voltage_pin1);
13   Serial.println(voltage_pin1);
14 }
```

Code listing 1: Voltage readings using Arduino

If the value of the resistor needed is calculated, the operational limits of the electrolyser and the analog pins must be taken into account, where the electrolyser limits defined by the manufacturer at a maximum of 2 [V] and 1.5 [A], and the maximum readable voltage with the Arduino analog pins can rise up to 5 [V]V. Due to the voltage limits, the minimum voltage drop across the resistor can be 5-2 = 3 [V]. Moreover, this minimum range would happen when the electrolyser is working at maximum power, meaning that the current flowing would be maximum and so the resistor value order of magnitude must be lower than $3[V]/1.5 [A] = 2 [\Omega]$. Due to the low resistor needed, and considering the

resistance of the cables, it is not possible to assure proper measurement readings with low oscillations.

The solution found to have precise voltage and current readings is the use of the module INA219 manufactured by Texas Instruments, which can read up to 26 [V] and 3.2 [A]. Moreover, the module is provided with a 12 bits ADC and different configurations can be set in order to lower the voltage and current ranges to measure. The connection between the Arduino 101 and the INA219 is performed by I2C interface instead of using the analog pins as before.

When the purchased INA219 module arrived, its connection with the Arduino 101 is made through the usual pins of this type of modules. However, the pin headers were not soldered to the module itself and it was necessary to use the tin solder shown in figure 12 to make a proper solder pin header connection to ensure a good communication.
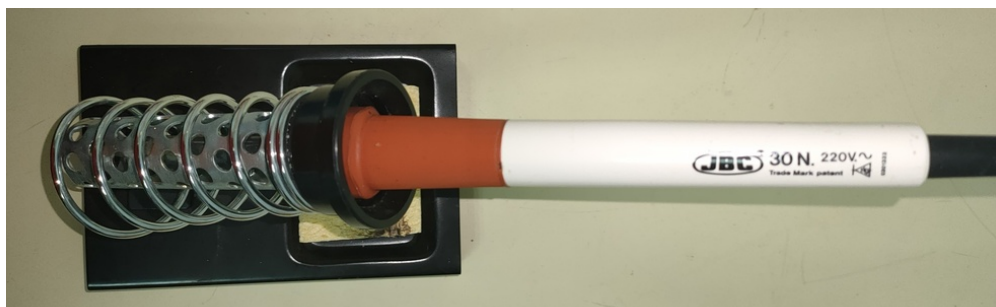
Figure 12: Tin solder - JBC brand

The wiring needed is shown in figure 13, where the INA219 is placed in series between the power supply and the electrolyser cell circuit. Moreover, four pins are connected between the Arduino 101 and the INA219, the red and black ones are used for power purposes, while the orange and purple are for data transmission by the SCL and SDA pins, respectively. Additionally, the Arduino 101, INA219 and power supply grounds are all connected together so no differences in voltages are set, which could lead to possible offsets in the readings.
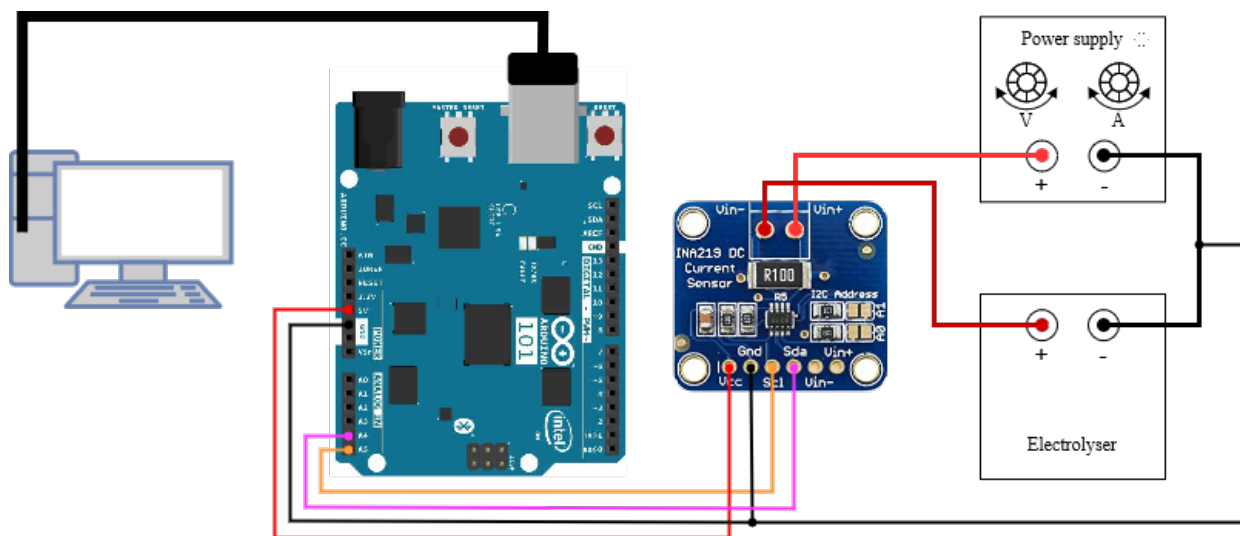
Figure 13: Wiring schematic for voltage and current readings with INA219

For programming the INA219, the library "Adafruit INA219 by Adafruit" [18] has been used, so the previous installation of the library is needed. The "Wire" library, which allow the Arduino 101 to communicate by the I2C interface, is not needed to be installed as it is usually included by default in the Arduino environment.

However, there exist a factory error when using the Intel Curie base library's "Wire" because it does not define the function "end()". The solution found is to manually add "void end()" at the bottom of the "TwoWire" function which is located in the Wire.h file. The file is placed, by default, in the route: *C:\Users\user\AppData\Local\Arduino\packages\Intel\ hardware\arc32\2.0.6\libraries\Wire\src*.

Once the wiring has been connected and the library installed correctly, is proceeded to generate the code in Arduino that allows reading the measurements of the INA219 module. In the following list of code 2 an example is detailed, where in the first lines the necessary libraries and the declaration of a variable that defines the module itself are included. During the setup function, the serial port that allows communication between the Arduino 101 board and the computer is initialized, and the calibration wanted the INA219 module is defined. There are three different calibrations that allow alternating the limits of the voltage and current to be measured, and therefore also the resolution of the data taken. Since the number of bits in the ADC is fixed, the higher the limit of the variable to be measured, the lower the available resolution. The available limits are 32 or 16 [V] and 1, 2 or 3.2 [A], where in the particular case of the electrolyser, it has been decided to establish the calibration at 16 V and 2 [A].

In the void function, the variables that will store any value read from the INA219 module are initialized to later take the measurements thanks to the functions already defined in the Adafruit library, and the code finally display the measurements read on the screen.

```
1  #include <Wire.h>
2  #include <Adafruit_INA219.h>
3
4  Adafruit_INA219 ina219;
5
6  void setup(void)
7  {
8    Serial.begin(9600);
9    }
10   ina219.setCalibration_16V_2A();
11 }
12
13 void loop(void)
14 {
15   float shuntvoltage = 0;
16   float busvoltage = 0;
17   float current_mA = 0;
18   float loadvoltage = 0;
19
20   shuntvoltage = ina219.getShuntVoltage_mV();
21   busvoltage = ina219.getBusVoltage_V();
22   current_mA = ina219.getCurrent_mA();
23   loadvoltage = busvoltage + (shuntvoltage / 1000);
24
25   Serial.print("electrolyser - Voltage = ");
```

```
26   Serial.print(loadvoltage);
27   Serial.print(" V, Current = ");
28   Serial.print(current_mA);
29   Serial.println(" mV");
30
31   delay(2000);
32 }
33 }
```

Code listing 2: Voltage and current readings using INA219

The voltage and current measurements read are necessary to be checked if the values that are being taken are real, calibrated and sufficiently accurate. The power supply used is the Promax FAC-363 that can be seen in the figure 14, which has manual adjustments by means of two potentiometers for both voltage and current, with a resolution of 0.1 [V] and 0.01 [A].

Figure 14: Power Supply - Promax FAC-363

On the other hand, due to the calibration that has been established in the INA219 module of 16 [V] and 2 [A] the available resolution when measuring the voltage and current is 0.01 [V] and 0.004 [A]. For that reason, the INA219 resolution is better than the power supply resolution. To calibrate the measurements taken with the INA219, a certified calibrated device with a better resolution than the INA219 is needed. The Kaise MY63 multimeter shown in the figure 15 has been used, which resolution is of 0.01 [V] and 0.001 [A].

ETSEIB

Figure 15: Multimeter - Kaise MY63

When calibrating the measurements taken by the INA219 module using the multimeter, the importance of the connection between the negative terminal of the power supply, the INA219 module itself and the Arduino board that has been previously shown in the figure 13 has been verified since in this way the same potential is taken as a reference for all the elements. After checking the calibration of the INA219 module using the Kaise MY63 multimeter, it has been established that the INA219 module is perfectly calibrated, having perfect linearity. If the connection between the negative terminals of the power supply, the INA219 module and the Arduino 101 was not made, the negative potential that the INA219 module would measure, would be established by the serial cable that connects the Arduino to the computer. While the positive terminal that the INA219 module would measure, would correspond to the one established by the power supply, resulting in a potential difference measured by the INA219 module that would need a calibration, mainly the addition of an offset.

3.3   Temperature using thermocouples

The thermocouple sensor works with the Seebeck effect, which states that a temperature difference in a junction made of two metals can be correlated with a difference in the voltage across the junction. However, the existing voltage in the junction is very small for the Arduino to be measured and a module which amplifies de voltage is needed.

The module used is the MAX31855 which can measure the voltage between the thermocouple terminals, amplify it and convert it to a digital output using a 12 bits ADC. The thermocouple type used is "K", which are the most common ones, the temperature working range is between -200 °C and 1250 °C, and so the available resolution is $\pm$ 0.25 °C.

The wiring schematic of the MAX31855 module is presented in figure 16, where the yellow

and blue wires represent the thermocouple terminals, the red and black wires are used for the power supply of the module; and the pink, orange and green wires are referred to the digital output (DO), chip selector (CS) and internal clock (CLK) of the module respectively.
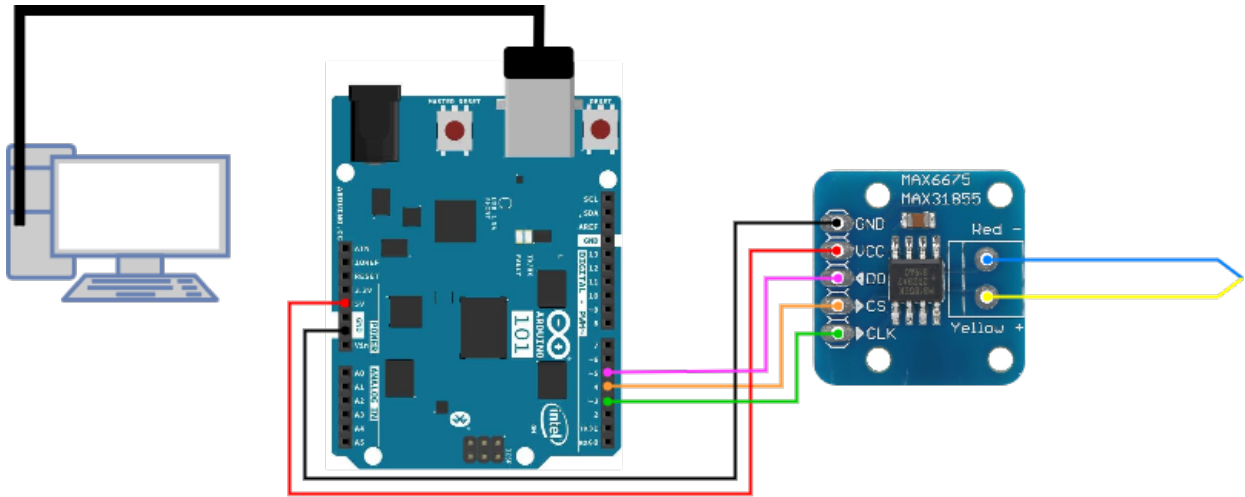
Figure 16: Wiring schematic for temperature reading with MAX31855

A basic example of the Arduino code needed to measure the temperature using a thermocuople and the MAX31855 module is presented in the following code listing 3, for which the corresponding Adafruit library has been used. At the top of the listing, the Arduino pin numbers are defined for the connections with the module as constants, being used to define the thermocouple object in line 5.

In the set up function, the serial port and the thermocouple are initialized and in the loop function the thermocouple temperature, read in Celsius, is measured and stored in the "temp" variable. If there exist any fault in the thermocouple, the origin of the error is found through the "read.Error" function, being possible three different causes: the thermocouple is not connected, it is short circuited to ground or it is short circuited to the positive terminal of the power supply. Finally, the measured temperature is printed in the console.

```
1  #define MAXDO    3
2  #define MAXCS    4
3  #define MAXCLK   5
4
5  Adafruit_MAX31855 thermocouple(MAXCLK, MAXCS, MAXDO);
6
7  void setup() {
8    Serial.begin(9600);
9    delay(500);
10
11   Serial.print("Initializing sensor...");
12   if (!thermocouple.begin()) {
13     Serial.println("ERROR.");
14     while (1) delay(10);
15   }
16   Serial.println("DONE.");
```

ETSEIB

```
17 }
18
19 void loop() {
20     double c = thermocouple.readCelsius();
21     if (isnan(c)) {
22       Serial.println("Thermocouple␣fault(s)␣detected!");
23       uint8_t e = thermocouple.readError();
24       if (e & MAX31855_FAULT_OPEN) Serial.println("FAULT:␣Thermocouple␣is␣open␣
             -␣no␣connections.");
25       if (e & MAX31855_FAULT_SHORT_GND) Serial.println("FAULT:␣Thermocouple␣is␣
             short-circuited␣to␣GND.");
26       if (e & MAX31855_FAULT_SHORT_VCC) Serial.println("FAULT:␣Thermocouple␣is␣
             short-circuited␣to␣VCC.");
27     } else {
28       Serial.print("C␣=␣");
29       Serial.println(c);
30     }
31     delay(1000);
32 }
```

Code listing 3: Temperature reading using MAX31855

As there exist temperature gradients all across the electrolyser assembly in all directions, the more temperature points can be measured the better. However, in this project it has been decided to focus in three main points in the electrolyser assembly: inlet liquid water, output oxygen gas and output hydrogen gas. For that reason, at the beginning of the project four MAX31855 were bought, where three of them could be used and there would exist one more in case of needing a replacement.

As explained above, each MAX31855 needs five pin connections with the Arduino board to measure the temperature of one point in the electrolyser. However, the Arduino board does not have enough pins to connect all the necessary pins of the three modules, with a total of 15 pins, where each one has specific requirements. To solve this problem, it has been decided to group the signals of the pins that are not critical.

Of the five pins that each MAX31855 module needs to work, the critical pin corresponds to the DO, since it communicates with the arduino board to return the digital value of the temperature measurement. As the signals from the other four pins are not critical, they have been grouped together, resulting in one output pin of the Arduino board being connected to the input pins of several MAX31855 modules, thus solving the pin shortage problem.

In the following figure 17 the wiring diagram when several modules are connected can be observed, where a protoboard has been used to group the pins. In this way all the black, red, orange and green wires refer to the shared signals of the negative and positive power supply, the CLK and the CS, respectively. The pink cables, where each one has a different darkness, refer to the DO signals of each of the MAX31855 modules, which, as already explained, are independent.

ETSEIB
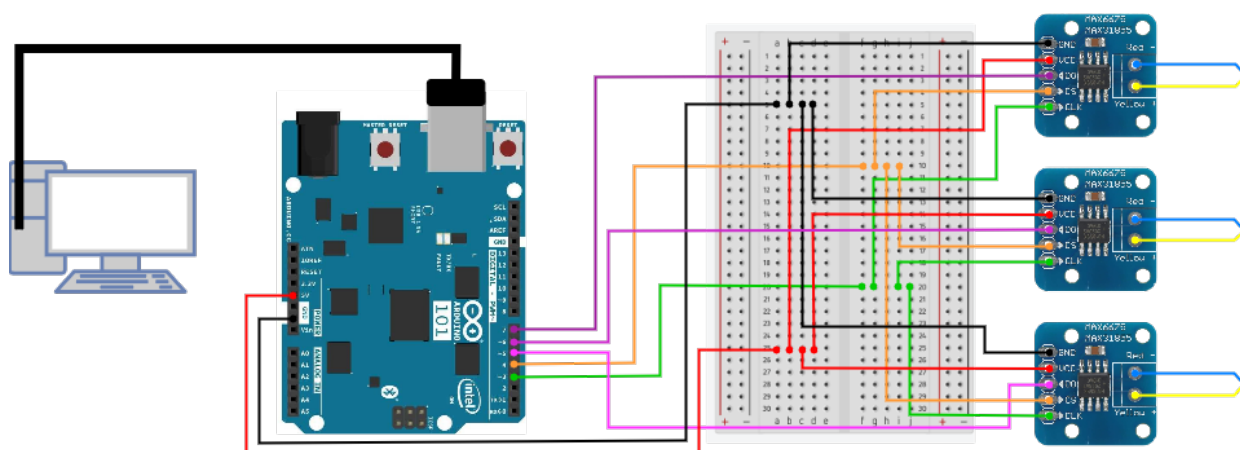
Figure 17: Wiring schematic for temperature reading with several MAX31855

The 4 MAX1855 modules were purchased from two different suppliers, having purchased a pair from each of the suppliers. Although during the start-up and the first experimental tests all the modules worked correctly, later the modules bought from a supplier began to give errors and finally stopped working. Due to the time constraint of this project, there was not enough time to buy some new extra MAX31855 modules to arrive on time. For this reason, it was finally decided to install the two available thermocouples, one at the water inlet to the electrolyser and the other at the oxygen outlet.

The thermocouples used have been those available in the laboratory that meet the requirement of being able to measure temperatures of a liquid. For this reason, the thermocouples have been used whose junction is covered with an insulating material, called inconel, to avoid the generation of a short circuit in the thermocouple. In the figure 18 one of these thermocouples is shown, whose junction is relatively long. However, when carrying out the first tests it was possible to verify that it was capable of measuring the temperature of a liquid or a solid when only the last millimeters of the thermocouple were exposed.

Figure 18: Thermocouple covered with inconel

After carrying out the wiring and the necessary programming, temperature measurements with the thermocouples were performed. However, the calibration of the measurements is necessary to ensure that the readings taken are real and accurate. For this reason, the Kosmon brand calibration oven shown in figure 19 is used, which allows establishing and knowing the temperature of a sand-filled capsule with a resolution of $\pm 0.1°$C. By inserting the thermocouples into the sand, the values measured by the thermocouples and the values defined by the calibration oven are compared.

ETSEIB

Figure 19: Calibration oven - Kosmon brand

To install the thermocouples in the most appropriate position, two possibilities were evaluated. The first option consisted of bending the thermocouples at an angle of 90°, and introducing them through the accumulator to the inlet and outlet tubes of the electrolyser, so that a large part of the thermocouple is submerged in the inlet water. The second option was to puncture the inlet water rubber tubes and outlet oxygen to the electrolyser so that the last millimeters of the thermocouple were inside the tube, leaving most of it in contact with the environment.

In a short test, it was proven that the thermocouples were capable of making a correct measurement when only the last few millimeters in the end were in contact with a hot source on one side. And to prevent the temperature gradient in the accumulator from distorting the temperature measurement, which is wanted to be as close as possible to the electrolyser, it was decided to opt for the installation of thermocouples by perforating the rubber tubes and inserting the end of the thermocouples.

When operating the electrolyser with the thermocouples installed, it was possible to verify that the tightening of the rubber tube itself on the thermocouple was not enough to prevent the leakage of water due to its hydrostatic pressure. For this reason it was necessary to apply a silicone sealant, which after drying prevents water leakage. The silicone used is from the Ceys brand, whose recommended uses are for bathrooms, kitchens or humid environments, and withstanding temperatures up to 120°C. Once the thermocouple is installed in a pipe and the silicone applied, the assembly remains as shown in the figure 20.

Figure 20: Thermmocouple installed in pipe

3.4 Temperature using a thermal imaging camera

The temperature gradient in the electrolysis cell is impossible to measure using commercial thermocouples due to the dimensions of the elements, bearing in mind that the usual membrane thickness has an order of magnitude of micrometers.

The electolyser cell used is composed by two metal grillages whose function is to provide the electrons and potential needed for the reaction to happen, and so both grillages are connected to the power supply. The structural material is constituted of two plates made of methacrylate, creating a sealed sandwich including the MEA and grillages. Thanks to the fact that the structural material is methacrylate, the use of a thermal imaging camera is expected to provide information of the temperatures variations in the electrolyser cell.

Moreover, during the electrolyser operation, the inlet water can be at different temperatures and the electrochemical reaction produces heat as well. Monitoring the gradients involved in the different components would need to include a large amount of thermocouples, and the thermal image camera can provide information about the gradients occurring in the different elements of the electrolyser.

The thermal imaging camera perceives the infrared radiation of the different objects, and due to the fact that there exist a correlation between an object temperature and its infrared radiation, the camera provides the temperature image of the surrounding objects. In the electrolyser cell, the components with a higher temperature and the heat generation are encapsulated inside the methacrylates plates, pipes or accumulators. For the thermal imaging camera to perceive the infrared radiation, it must cross the methacrylate, and so the methacrylate infrared transmittance must be taken into account.

The infrared transmittance of an object refers to the ratio between the incident radiation and the reflected radiation. The transmittance must be taken into consideration because if a heat generation is captured with the thermal imaging camera having a low transmit-

ETSEIB

tance material in between, the temperature captured and associated to the object won't be realistic and will always be much lower than the actual temperature of the object.

There are currently numerous types methacrylates available on the market with different transmittances depending on their uses. However, the most widely used methacrylate, which is transparent to visible light, has a transmittance of 93% for visible light and allows infrared radiation to pass through it up to wavelengths of 2.5 [nm]. The specific data of the methacrylate used by the manufacturer is unknown, and therefore it will be assumed that the methacrylate used has these characteristics.

The camera available in the laboratory is from the Fluke brand, specifically the 480 Ti Pro model that is shown in figure 21, which is capable of measuring in a temperature range between -10°C and 1000°C for which it uses a sensor with an infrared spectral band between 7.5 and 14 [μm], that is, working within the long-wave infrared (LWIR) spectrum.

(a) Side view   (b) Front view

Figure 21: Thermal imaging camera - Fluke 480TiPro

Due to the wavelength mismatch between the methacrylate transparency and camera sensor, it is not possible to obtain temperature data from the grillages, since short-wave infrared radiation is not capable of passing through the methacrylate. However, both the inlet water -if it is at a higher temperature than the methacrylate- and the heat generated during the reaction will gradually heat the methacrylate through thermal conduction and the temperature that the camera will capture will be that of the methacrylate plate itself.

The first tests carried out with the thermal image camera in the laboratory were carried out when the daylight was falling through the windows, and a problem was found. Although the objective is to use the camera to capture the radiation emitted by the objects caused by its own temperature, the sunlight coming through the windows distorted the image that was displayed. Sunlight has visible, ultraviolet and infrared light spectrum.

When capturing the image of an object with the thermal camera in broad daylight, the sunlight reflected on the object was also captured by the camera, resulting in the image indicating a temperature of the object higher than the actual temperature. On the other hand, some electronic equipment such as computers, screens or the power supply that feeds the electrolyser are also at a higher temperature than the environment, and emit infrared radiation that could distort the image captured by the thermal imaging camera.

To solve these problems, the laboratory windows were covered by curtains and the black box that can be seen in figure 22 was made to place the electrolyser while the experimentation phase is carried out. Outside the black box would be the components that emit radiation such as the computer or the power supply. This black box was manufactured using the existing shelves in the laboratory, exhaustively covering all the gaps with tape to prevent the possible entry of light, and being covered with a thick black sailcloth for easy access to the area where the electrolyser is located. Once the black box was manufactured, the thermal image camera was used to check if there was radiation entering the box that could distort future measurement taking.

Figure 22: Black box

3.5 Water bath

In order to study the electrolyser behavior at different operating temperatures, it is necessary to be able to heat the inlet water. Although the use of previously heated water that is poured into the accumulator for its operation could be considered, the existing losses with the environment would cause that as the experimentation time elapses, the temperature of the inlet water decreases and therefore the temperature is not kept constant.

In order to keep the temperature of the inlet water constant, the thermal bath of the Ps-electa brand has been used, which can be seen in the figure 23, which has a pump that provides a flow rate of 12 [l/min] and a resistance of 2 [kW] that allows heating the water

up to a temperature of approximately 100 °C.

Figure 23: Water bath - Pselecta brand

Although it has been decided to use a water bath to keep the water at a constant temperature, its use involves two other drawbacks. The first one is that the electrolyser uses pure water for its operation, and due to previous uses of the water bath, it has numerous impurities in its components. After having carried out a general cleaning, it has been verified that it has numerous nooks that would have to be cleaned, disassembling the components to prevent the water entering the electrolyser having impurities. After having done the general cleaning, you can see some existing impurities in the image 24.

Figure 24: Water bath impurities

The second drawback is that the thermal bath has a hydraulic pump that would make the water to flow at the desired temperature from the water bath tank to the electrolyser accumulator. However, it would be necessary to install a return circuit that makes the water

flow back to the water bath tank, necessitating the installation of an additional hydraulic pump.

Due to these two drawbacks, it has been decided to use a heat exchanger that would be inside the electrolyser inlet water accumulator. In this way, the impure water from the water bath would not be the same and would not mixed with the inlet water to the electrolyser. Moreover, the use of any additional hydraulic pump would not be needed, since the water bath pump itself would make the water flow through the heat exchanger and returning the water back to the water bath tank. However, the use of this system means that the temperature of the water in the accumulator is lower than the water in the water bath tank.

The heat exchanger to be installed inside the accumulator must have very specific characteristics for its use. The most important are that it must have small dimensions to be able to fit inside the accumulator and that both the entrance and the exit must be in the same place -at the top- because the accumulator is only opened in its upper part.

After searching for suitable heat exchangers on the market that could arrive on time for use in this project whose time extension is limited, none was found that met these premises. For this reason, it was decided to manufacture the heat exchanger. To do this, a copper tube was used, shaping it to the desired design. As the rubber tubes that would connect the manufactured heat exchanger to the water bath circuit have an internal diameter of 4.5 [mm], the copper tube that was purchased had an external diameter of 5 [mm] so that there would be a small compression that held them together. But the most suitable dimensions of copper tube wall, which also define the internal diameter of the tube, were unknown. The importance of these walls lies not only in the definition of the internal diameter through which the water will flow, the amount of thermal resistance existing between the water flowing and the water in the accumulator, but also in the force necessary to bend the tube when shaping the heat exchanger. As the ideal tube wall was unknown, two different copper tubes were purchased, with wall thicknesses of 0.5 and 1 [mm].

When shaping the copper tube, it is necessary to make a very closed curve, which might generate the tube itself to break, or that the walls collapse due to the lack of material inside. To avoid this behaviour, and following the recommendations of a plumber, salt grains were put inside the tube before deforming it. After having filled the tube with salt and closed both ends, when deforming the tube, the salt prevents the walls from collapsing by serving as internal support. Despite using the salt, the 0.5 [mm] wall tube did not withstand the deformation generated when shaping the necessary turns and broke. Using the 1 [mm] wall tube, it was possible to manufacture the heat exchanger shown in the figure 25 and finally the salt was extracted once the desired final shape was achieved.

Figure 25: Heat exchanger

The heat exchanger has been held with laboratory grip stand, as shown in figure 26a, to maintain its position inside the accumulator as can be seen in figure 26b.
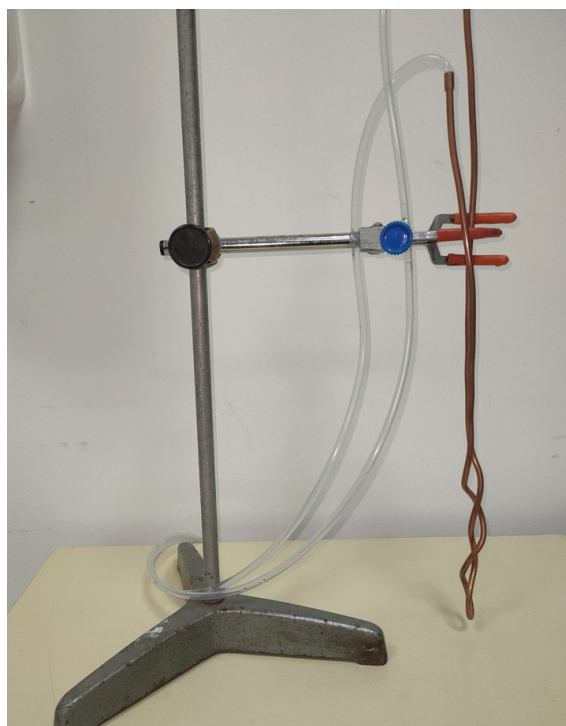
(a) Heat exchanger held by grip stand

(b) Heat exchanger placed in the accumulator

Figure 26: Heat exchanger position

Once the heat exchanger has been manufactured, placed inside the inlet water accumulator and the tubes that connect the water bath with the heat exchanger to make the water flow properly; the system has been star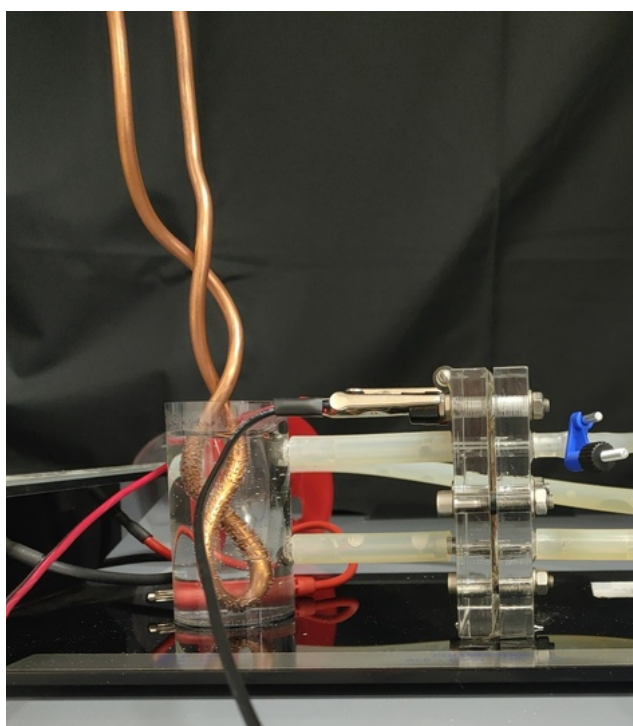ted up to check the temperature that can be achieved in the inlet water with approximately 100°C in the water from the thermal bath tank. In the images of figure 27 the evolution of the temperature of the tank and the electrolyser can be observed when the water bath was started. Every half hour an image of the system has been taken with the thermal camera and finally it has been observed that the image made at 90 and 120 minutes have the same temperature, for this reason the system takes an hour and a half to reach the stationary state. After making the images, the same color scale has been established in all the images, being 21°C in the coldest colors (dark blues) and 55°C in the warmest colors (red/white).
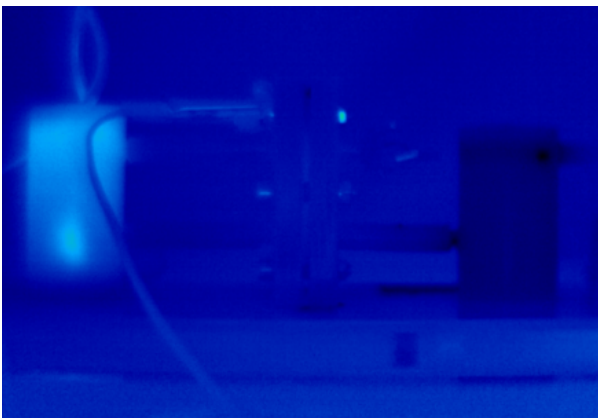
(a) 30 min heating time
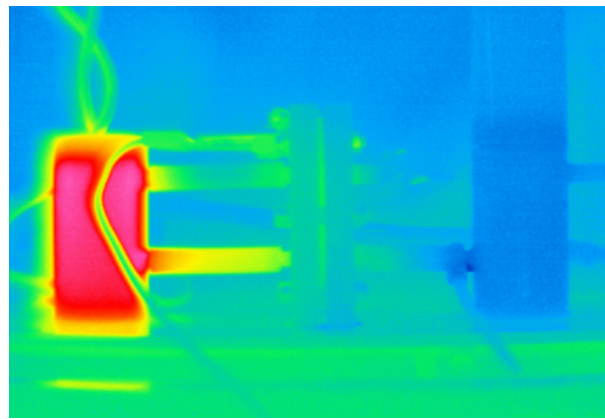
(b) 60 min heating time
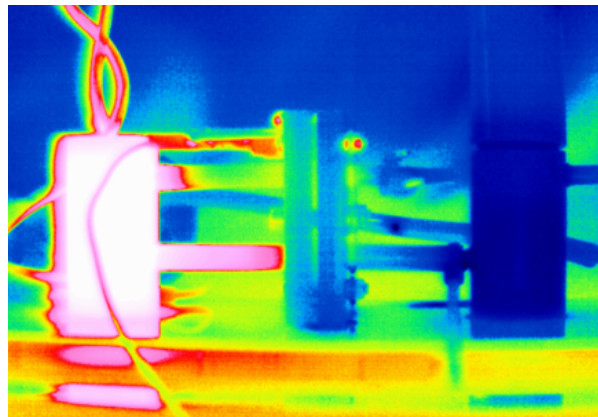
(c) 90 min heating time

Figure 27: Heating of the electrolyser inlet water

However, with the configuration mentioned, despite having the water in the water bath at a temperature close to 100°C, the temperature of the water at the entrance to the electrolyser is 35°C. This great temperature variation is mainly due to the losses with the environment existing in the entire hydraulic circuit, both in the rubber pipes that connect the water bath with the heat exchanger, as well as in the heat exchanger itself, in the accumulator and in the water inlet pipe to the electrolyser. The radiation emitted by the heated components is reflected and it seems that the electrolyser base is heated when it is not. This behaviour is exactly the same alteration that happened with the sunlight before the black box was assembled.

ETSEIB

In addition, when the thermocouple is installed, it dissipates heat with the environment acting as a fin. In the figure 28 it can be observed thanks to the thermal imaging camera, how the water heats the thermocouple, increasing its temperature due to thermal conduction, exchanging heat with the environment.
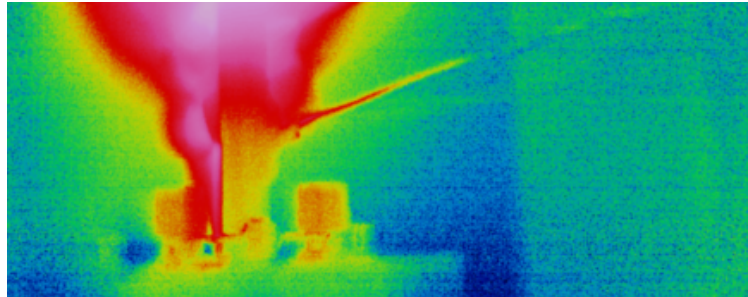
Figure 28: Thermocouple dissipating heat

In order to minimize thermal losses and achieve higher inlet water temperatures at a higher temperature have been insulated. Insulating foam has been used to wrap the entire circuit of the heat exchanger, the accumulator and the inlet pipe to the electrolyser, as shown in the figure 29.
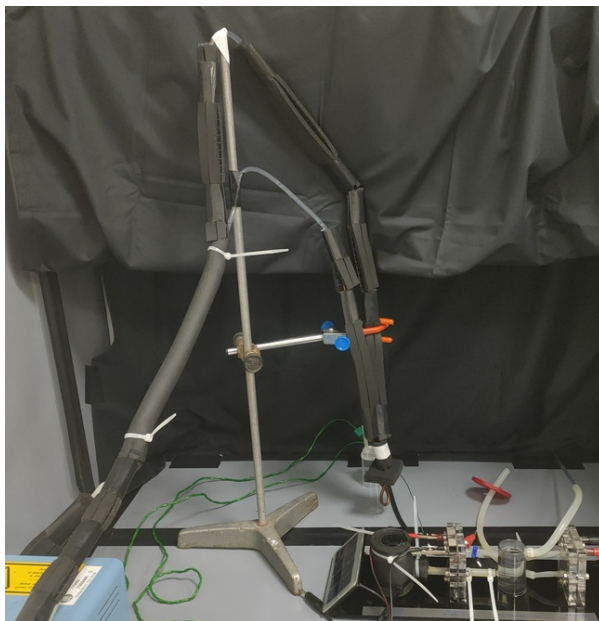
(a) Water bath circuit
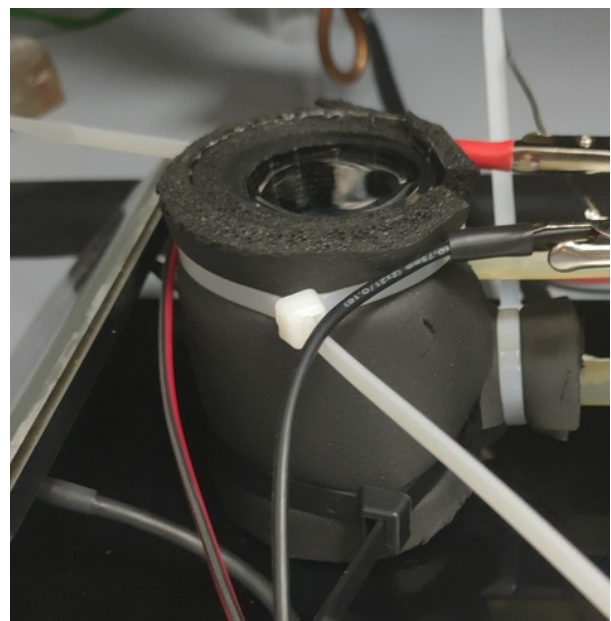
(b) Inlet water accumulator

(c) Thermocouple

Figure 29: Insulation foam installation

After isolating the system, it has been possible to have a temperature of 60 °C at the en-

trance of the electrolyser, therefore, during the experimentation phase, tests will be carried out within the temperature range from ambient temperature to 60 °C.

3.6 Hydrogen production

Another of the variables to monitor during the electrolyser operation is the amount of hydrogen produced, thus making it possible to know the electrolysis efficiency by previously knowing the energy (voltage and current) that is being supplied.

As shown in the figure 5, the hydrogen produced in the electrolyser flows through its tube until it reaches the hydrogen accumulator. The hydrogen accumulator is filled with water but due to the connection with upper accumulator, the hydrogen produced is accumulated in the accumulator, and while it is being filled, the water is displaced through the connection between both accumulators. On the other hand, the hydrogen accumulator has an outlet at the top that allows the hydrogen to be introduced into the fuel cell to recombine with atmospheric air oxygen, generating electricity and producing water.

The first proposal made to quantify the hydrogen production while the rest of the system continues to function in a similar way is the following. The CAD design of an upper cap was made, shown in the figure 30, which has two through holes and a notch for the inclusion of a gasket that ensures its tightness with the hydrogen accumulator. A laboratory pipet is attached to one of the two holes and a long rubber tube to the other hole. When producing hydrogen, it would enter the pipette, displacing the water in the accumulator, which could only leave through the rubber tube. Being able to measure the amount of hydrogen based on the difference in level of the water displaced in the pipette or in the rubber tube.
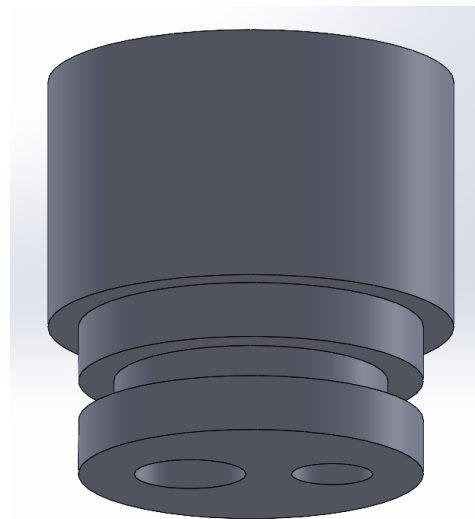
Figure 30: Hydrogen production cap design

The hydrogen produced enters the accumulator through a tube, forming a bubble that rises to its upper part, because the accumulator is full of liquid water and the hydrogen produced is in a gaseous state. For this reason it is necessary to ensure that the hydrogen bubble enters the pipet and that the rubber tube does not come out. The design of the

piece shown in figure 31 was created, which has a cone that collects the hydrogen bubble and whose outlet is connected to the lower part of the pipet hole. As it is necessary that the water can flow freely through the accumulator so that its level inside the rubber tube rises, in the upper part of the piece there are several holes that allow the flow of water.
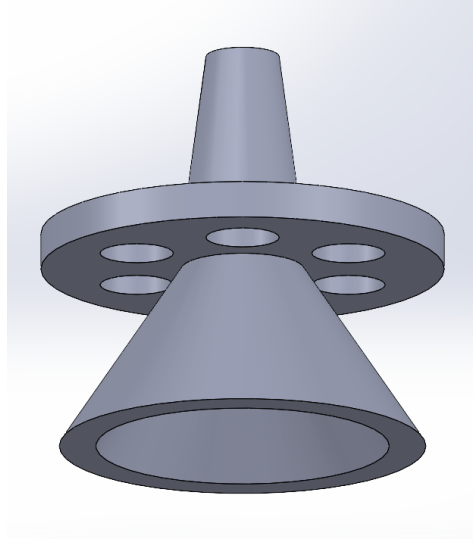
Figure 31: Hydrogen production cone design

After taking the real dimensions of the experimental accumulator with a caliper of the Mitutoyo that has a resolution of ± 0.05 [mm]. The manufacturing of both pieces is made by 3D printing using FDM (filament deposition modelling) method. It has been decided to use this manufacturing method due to the ease of access as the university has a manufacturing space, being able to have the designs manufactured in a short period of time. Once the parts were manufactured, it was necessary to cover the fitting area with Teflon tape to ensure a better fit and tightness, since the precision obtained during manufacturing with the 3D printer was not precise enough. In the figure 32 both finished pieces can be observed.
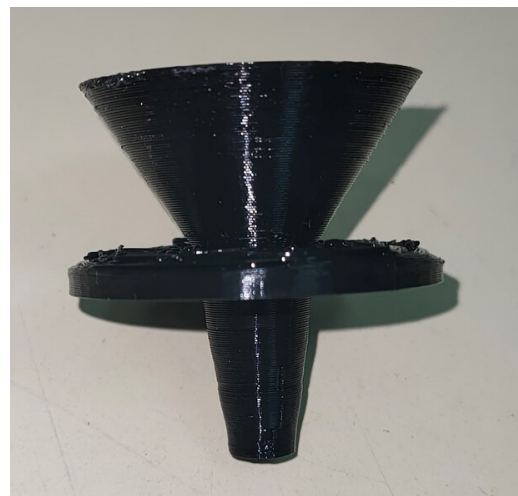
(a) Printed cap   (b) Printed cone

Figure 32: 3D printed cap, cone and assembly

The assembly formed by the designed and printed parts, together with the necessary rubber tubes and the pipet are shown in the following figure 33, where the cone would collect the hydrogen produced directing it into the pipet and the water in the accumulator could raise its level through the exhaust tube on the left.

Figure 33: Printed assembly

However, the use of these two pieces entails two problems that made the hydrogen production monitoring not possible. The first problem is due to the manufacturing process used, 3D printing. The manufacturing process consists of overlapped layers of filament to form the desired design. By not sculpting the design from a solid block, and because small gaps are generated between the layers of printed filament, there were leaks of water and hydrogen through the gaps in the piece itself. The second problem is caused by the fact that the pipet has a very small internal tube. When the hydrogen bubbles were generated, the hydrogen bubbles were directed into the pipet, dragging some water. Due to the small diameter of the inner pipet tube, the surface tension of the entrained liquid water kept the water rising through the pipet, being pushed by the generated hydrogen, preventing the little entrained water from falling into the accumulator by its own weight. In addition, sometimes the surface tension of the entrained drop of water broke, causing the drop to fall into the pipet, changing the level that was visually followed to measure the hydrogen production.

Finally, the solution adopted is the following. The tube connecting the hydrogen accumulator to the fuel cell is disconnected and in its place the pipette is connected with its upper

end open. Thanks to the availability of another experiment kit model that shares some similar components and the cap seen in figure 34 could be used. This cap adapts perfectly to the accumulator and is made from a methacrylate block, so the aforementioned leak problems do not appear in this solution.

Figure 34: Closed cap

When measuring the hydrogen production, the hydrogen storage tank is filled to the brim with water. By inserting the cap, the water flows through the tube without reaching the pipet. When the electrolyser starts operating, the generated hydrogen moves the water inside the tube until it reaches the pipette. Due to the length of the tube, along with being full of water, visualization problems do not exist in this solution because it is always possible to see the water level in the pipette because the hydrogen bubbles are in an area of the tube closer to the accumulator. After the hydrogen production has been measured once, it is necessary to open the cap to allow the hydrogen to flow out and the water level in the pipet to return to its initial value for further measurement. The accumulator assembly closed by the stopper and connected to the pipette by the tube can be seen in the figure 35.
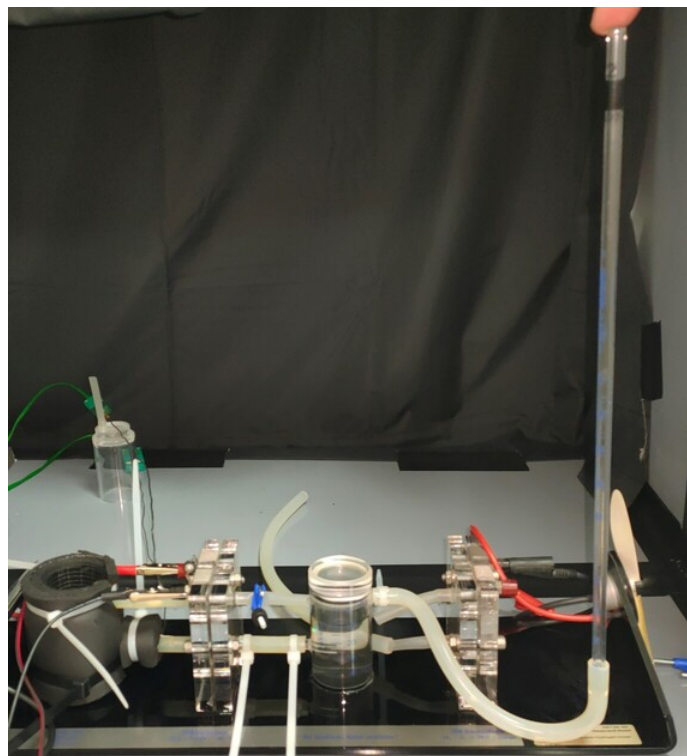
Figure 35: Hydrogen production monitoring assembly

ETSEIB

The experiment with all its components installed is the one shown in figure X. Where it can be observed the electrolyser inside the black box with the curtain up. The thermal bath is on the left, connected by its pipes to the heat exchanger that is inside the box to be positioned inside the inlet water accumulator. The MAX31855, INA219 modules, the Aarduino 101 board and the protoboard are located at the bottom of the image, relatively close to both the electrolyzer and the power supply (which is on the bottom shelves of the black box) to which it is connected the INA2A module.

Figure 36: Complete experiment assembly

3.7   Automation for long measurements periods

During the first tests carried out with the electrolyser and the different sensors, it was verified that the general behavior of the electrolyser was relatively fast. However, another behavior was also noticed, which will be presented in the results section, whose variation is very slow. The laboratory is located in a university facility where it can only be accessed during working hours, so carrying out long-term experiments is subject to complying with these schedules.

In order to perform long in time experiments, it is necessary to have some way allowing the data acquisition from the sensors to be saved while it is being generated. Currently, the Arduino code does not have a library or simple functions that allow an easy export of

ETSEIB

the measured data, as well as its saving. To solve this problem, and since the author had programming knowledge in Python, a small script has been coded in that language being able to capture the data sent by the Arduino 101.

The first step performed is the downloading and installation of the most up-to-date Python program. In addition, the Wing development environment has been downloaded too. It has been decided to use this development environment due to its simplicity, that it is free of charge, that it meets all the necessary requirements, and because the author already knew both its download process and its use.

After having all the necessary programs installed, it has also been necessary to install three libraries that will be used in the code. the first library is the "time" library, that allows creating delays in the code. The "serial" library allows the access and management of the serial port that serves as communication between the Arduino 101 and the computer. The last library needed to install is the "datetime" library, which is used to know the date of the device.

Once everything necessary has been arranged, the programming code shown in the 4 list has been generated. The script communicates with an Arduino device via a serial connection. It reads data from the Arduino, records it in a text file, and waits for a specific time interval before continuing the reading. The step-by-step breakdown is:

- **Lines 1-3:** The script imports the necessary libraries time and serial, and the function datetime.

- **Line 5:** It establishes a serial connection with the Arduino using the specified port and baud rate.

- **Lines 7-8:** After a brief delay to ensure a stable connection, the script enters a loop that will execute 1800 times.

- **Line 9:** Within the loop, it opens a file in append mode to write, and so store, the data.

- **Lines 10-13:** It reads a line of data from the Arduino and decodes it into a string. The script obtains the current date and time and formats it as a string. The date, time, and data is printed on the console so the behaviour of the script can also be followed in real time.

- **Lines 14-15:** The script writes the date, time, and data to the file. It waits for a short period to ensure a correct data writing in the file.

- **Lines 16-17:** After completing the loop, the file is closed, and the script waits for a longer interval before starting the process again.

In this specific case, the Arduino 101 sent the data every 30 seconds, and therefore the delay in line 17 is 29.75 seconds, which added to the other delay necessary to ensure correct storage of the information (in line 15) makes a total of 30 seconds. Depending on the sampling rate defined and the number of iterations established in the 'for' loop, the total data collection time is determined.

```python
import time
import serial
from datetime import datetime

serialArduino = serial.Serial('COM4',9600)

time.sleep(1)
for i in range (1800):
    archivo = open('C:/Users/termotecnia/Desktop/datos.txt', 'a')
    dat = serialArduino.readline().decode()
    dat = dat.rstrip('\n')
    dt = datetime.now().strftime("%d/%m/%Y \t %H:%M:%S \t")
    print(dt,' ',dat)
    archivo.write(dt + ' ' + dat)
    time.sleep(0.25)
    archivo.close()
    time.sleep(29.75)
```

Code listing 4: Python code used for storing data collected for long time

ETSEIB

4   Results

After having carried out all the previously explained work of installing the different sensors and data acquisition methods, it is proceeded to perform the different experiments to extract the data that will be presented in this section.

4.1   Electrolyser start-up

Although the graph obtained in previous literature (and shown in figure 6) does not show the first section of the polarization curve (between 0 [V] and 1.5 [V]), in this work it has been possible to find a relationship between two different variables. The first section of the polarization curve corresponds to the energy necessary to overcome the potential necessary for the reaction to occur. Theoretically, this potential should be 1.23 [V] under standard conditions, however, both in the literature curves and in those obtained experimentally in the laboratory, a value around 1.5 [V] has been found.

The polarization curve shown in the literature apparently the electrolyser does not consume any current until it is polarized. However, it has been found that during the start-up of the electrolyser, it does consume current before becoming polarized. In addition, the variation in current with which the electrolyser starts up affects not only the amount of current consumed, but also the value of the voltage with which it is possible to polarize the electrolyser. These results are shown in figure 37, where different polarization curves are presented during the start-up of the electrolyser applying different current rates.
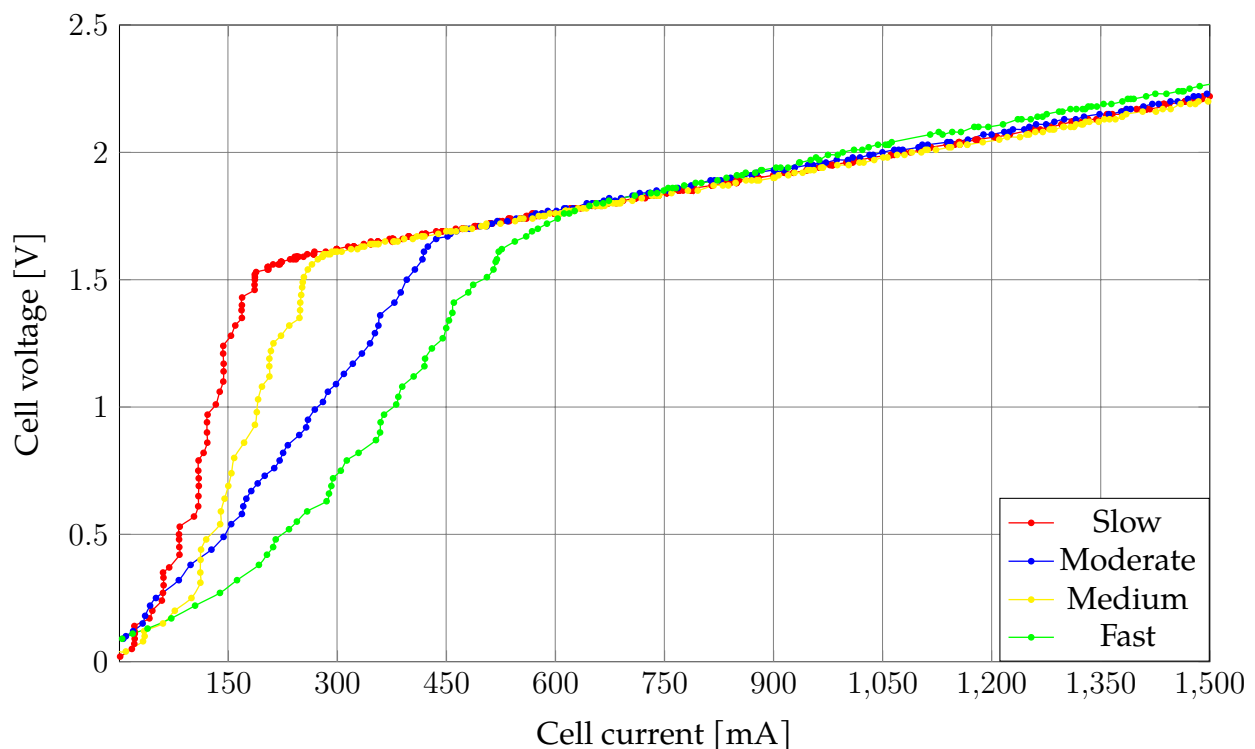
Figure 37: Polarization curves at different start-up current rates

The different current rates applied can be seen in the following figure 38. Its behavior is

intended to be as linear as possible, however the power supply is not programmable and the author has turned the potentiometer manually trying to make it as more stable and gradually as possible.
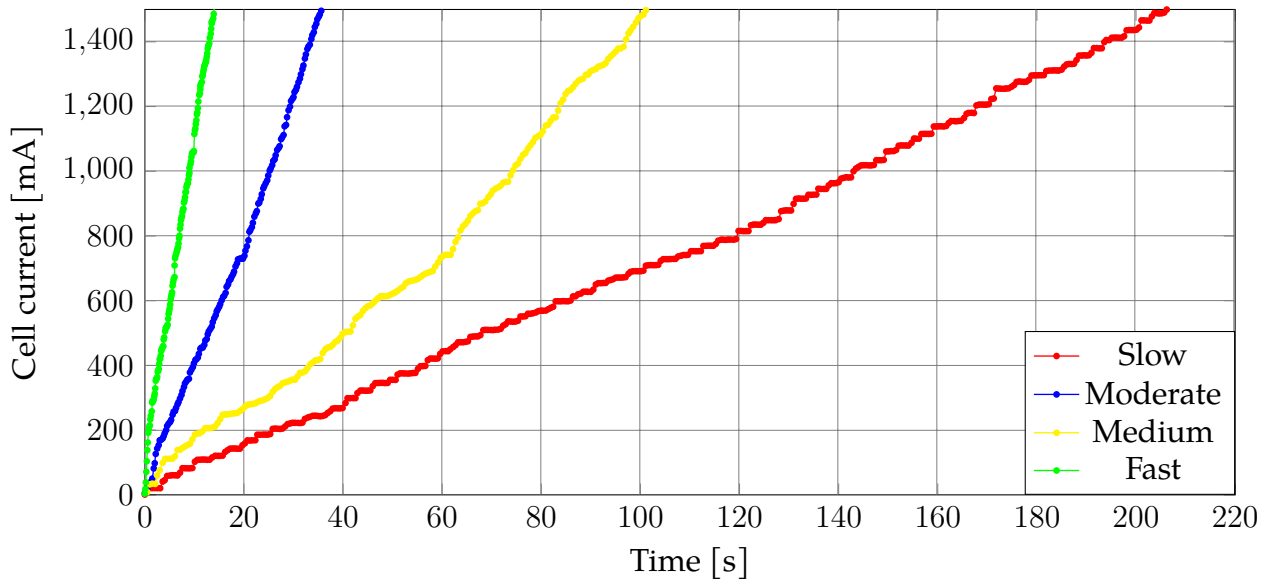
Figure 38: Current rates applied when starting-up the electrolyser

The evolution of the voltage for each current rate is shown in figure 39, where it can be seen how the voltage at which the electrolyser is polarized is considerably higher when the current rate is higher. It can be clearly observed in the graph how the slope change for each start-up line is at a different voltage value.
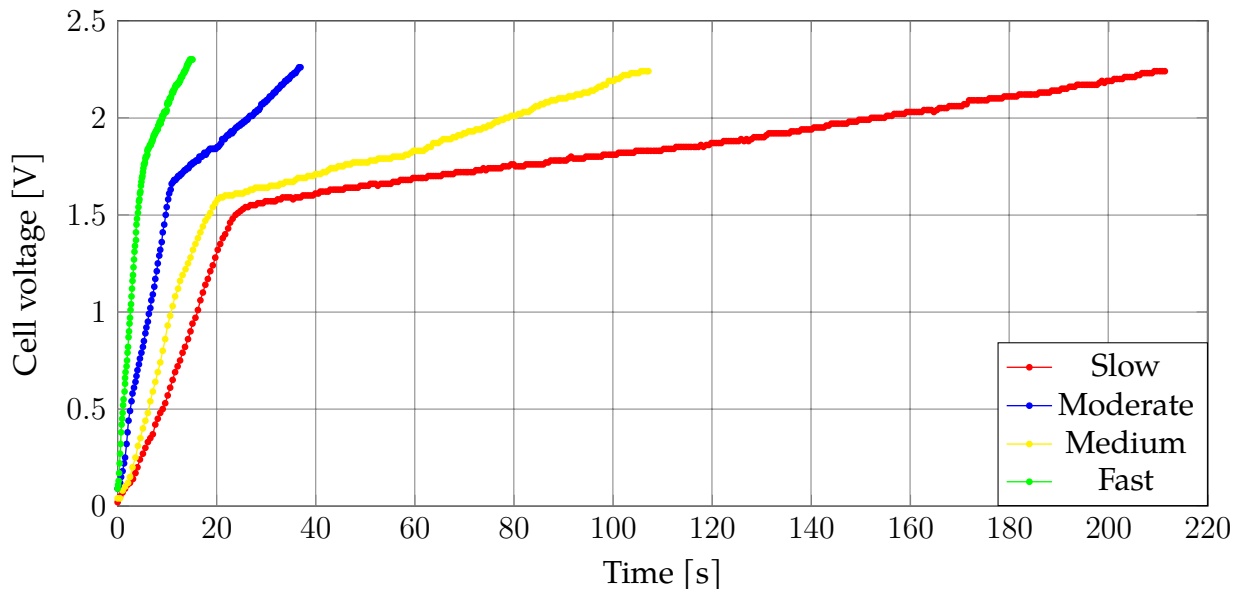
Figure 39: Voltage start-up at different current rates

4.2   Temperature effect on polarization curves and hydrogen production

The effect of the inlet water temperature on the polarization curve can be seen in the following figure 40, where it can be seen how the effect is minimal for small currents and increases for higher electrolyser working powers, forming the different lines a conical shape on the graph.
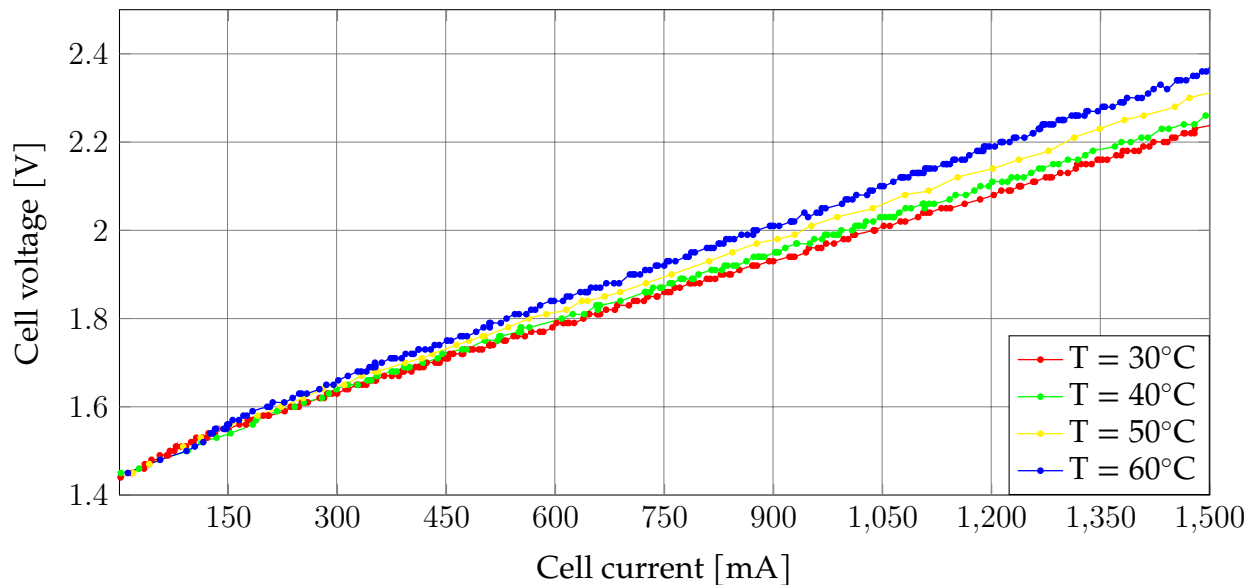
Figure 40: Polarization curve at different temperatures

The current provided to two different electrolysers with the same characteristics is linearly dependent on the MEA area and for this reason it is common for the graphs to provide the values of voltage and current density. By providing current density as a variable, two electrolysers with the same characteristics, except for the MEA area, would have the same polarization curve but obviously different electrical consumption and hydrogen production. The MEA of the electrolyser used has a square shape with sides of 4 [cm], giving as a result a surface area of 16 $[cm^2]$. In the figure 41 polarization curves for different temperatures as a function of voltage and current density in $[A/cm^2]$ can be observed. During the experimentation, the limit of 1.5 [A] established by the manufacturer has not been exceeded, and therefore the maximum current density obtained is approximately 0.1 $[A/cm^2]$. The electrolyser polarization curve shown in the figure 6 has a current density of up to 2 $[A/cm^2]$, being much higher than the studied electrolyser. This big difference is assumed to be caused by the difference in the characteristics of the electrolysers, where the one mentioned in the literature has an industrial use and the one used in this work has an academic demonstration use.
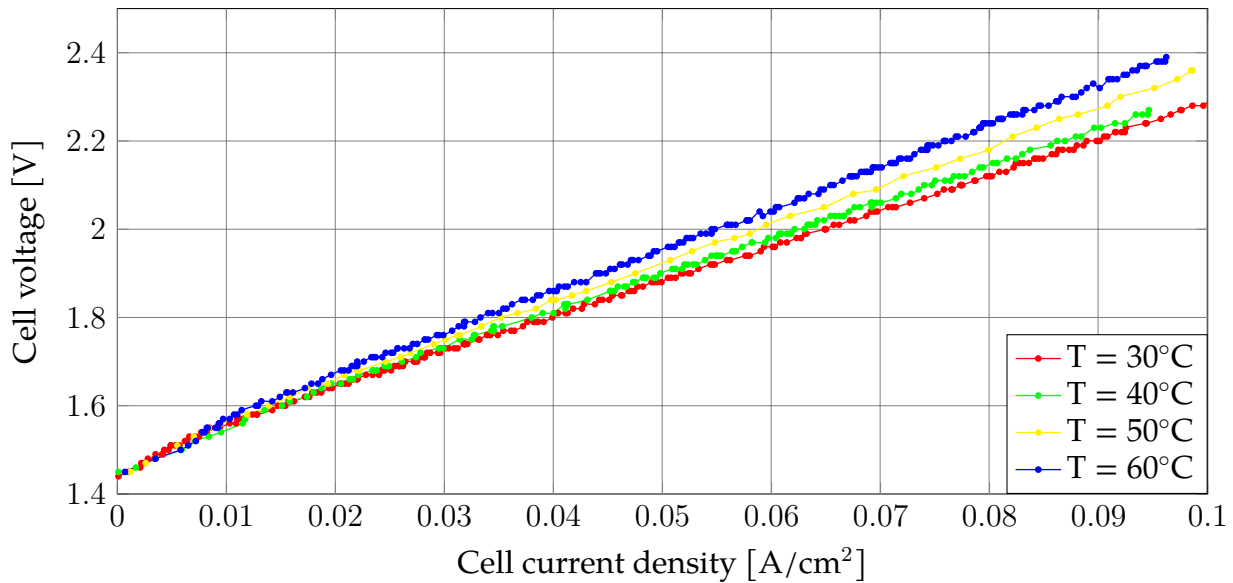
Figure 41: Polarization curve at different temperatures

The voltage efficiency of an electrolyser refers to the efficiency with which the applied voltage is used to generate hydrogen and oxygen when splitting water. It is calculated as the ratio between the actual applied voltage and the thermodynamic voltage required to carry out the electrolysis reaction. This difference is caused because in practice there are losses due to resistances and other inefficiencies of the system. The calculation of the voltage efficiency can be done using the following equation 34.

$$Voltage\ efficiency\ [\%] = \frac{Thermodynamic\ Voltage}{Actual\ Voltage} \cdot 100 \tag{34}$$

The thermodynamic voltage is determined using the standard cell potential for the water electrolysis reaction. Under standard conditions (25 °C and 1 atm), the standard cell potential of the water electrolysis reaction is approximately 1.23 [V]. The polarization curve starts at 1.44 [V] and ends at values close to 2.3 [V], depending on other factors such as temperature and mainly current density. Consequently, the calculated voltage efficiency is between 85.42% and 53.48% depending on the operating conditions.

Figure 42 shows the hydrogen production results at different temperatures, where no correlation has been found respect to temperature. The effect of temperature on hydrogen production seems to be negligible or the monitoring method is not appropriate.
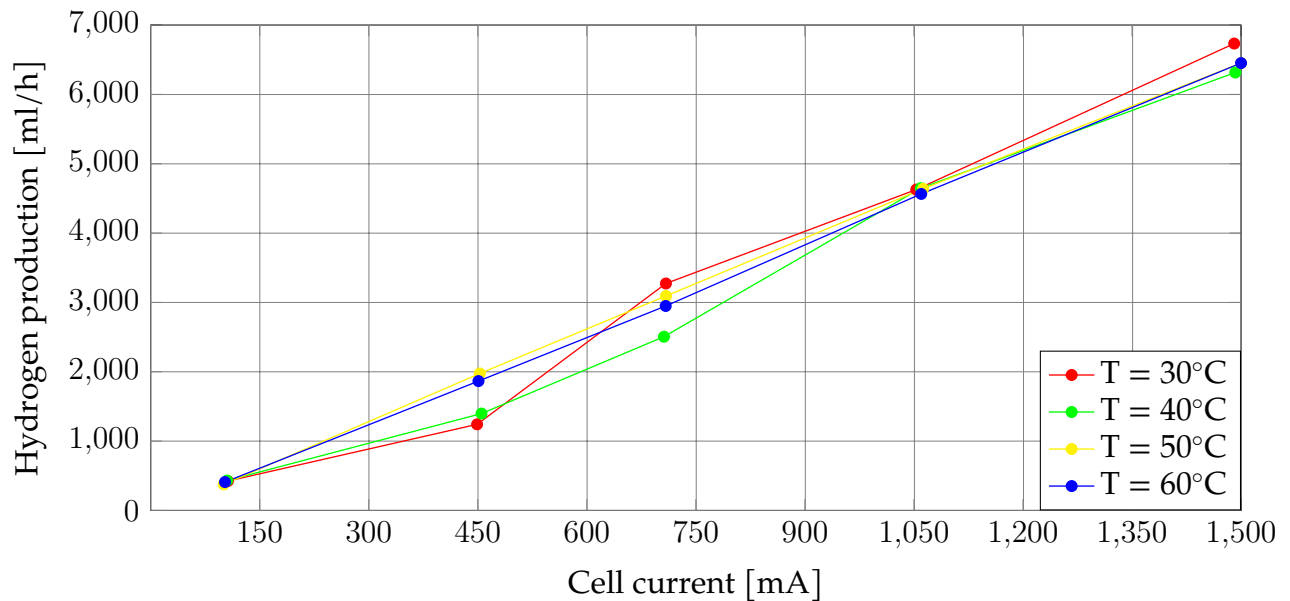
Figure 42: Hydrogen production at different temperatures

Regarding the data collection of the resulting voltages and currents during the experimentation stage, the time in which the electrolyser was working was about 10/15 minutes per experiment, and even a shorter period high current was flowing. However, during the hydrogen production data collection stage, the operating point of the electrolyser was maintained for a longer period of time due to the need to adjust the water level in the hydrogen accumulator, closing the cap and establishing a correct position of the pipet while avoiding the entrance of air bubbles inside the pipe that connects the accumulator to the pipet, keeping its entire interior filled with water. By maintaining relatively long periods of time with the electrolyser on, an oxygen bubble was observed coming out of the water inlet tube of the electrolyser. This phenomena is caused because the inlet water flow is not enough to drag the generated oxygen and maintain a correct and continuous inlet water flow to the electrolyser, along with insufficient oxygen output through its outlet pipe. The figure 43 shows the comparison between when the oxygen bubble exists and when the entire inlet tube is filled with liquid water.
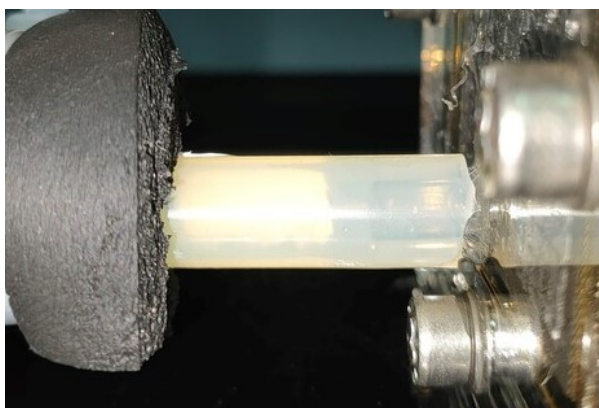
(a) No oxygen bubble in the inlet pipe   (b) Oxygen bubble in the inlet pipe
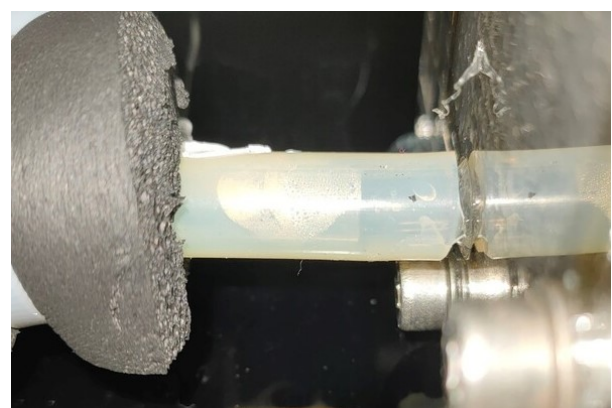
Figure 43: Oxygen bubble located in the water inlet pipe

Faraday efficiency is defined as the ratio between the amount of actual electrical charge used in the generation of hydrogen and the theoretical electrical charge required by the electrochemical reactions involved. Equation 35 describes how Faraday's efficiency can be calculated where the number 2 represents that two moles of electrons are needed to generate one mole of hydrogen, n_{H_2} refers to the actual production of moles of hydrogen, Q corresponds to the actual current used and F refers to Faraday's constant which has a value of 96.485 [s·A/mol].

$$Faradaic\ efficiency\ [\%] = \frac{2 \cdot n_{H_2}}{Q \cdot F} \cdot 100 \tag{35}$$

When calculating the Faraday efficiency using the results shown in figure 42, it is necessary first to convert the available hydrogen production in [ml/h] to [mol/s] values. So, a change of units is performed to obtain the production in [l/s] and finally the ideal gas equation is applied, from which it is extracted that a mole of ideal gas in standard conditions occupies a volume of 22.4 liters. After setting the hydrogen production in the proper units and applying the equation 35, approximate efficiencies of 1.1e-7 [%] are obtained, these values are very far from the expected, which should be between 40% and 80%. For this reason, it is considered that the impossibility of a correct oxygen outlet generates a bottleneck preventing water from entering the electrolyser correctly, and the lack of sufficient water for the reaction to take place.

4.3 Electrolyser voltage decay

When the electrolyser is stopped being fed, it is found that it maintains the voltage between its terminals because it is polarized. The voltage decays over time as shown by the red line in the graph in the figure 44. In addition, in the case of short-circuiting the terminals for a short period of time, it causes the value of the potential between the terminals to be zero, but it recovers part of that potential and continue decaying later. The existence of this voltage is assumed to be due to the remains of hydrogen and oxygen in the electrolyser, which spontaneously recombine when the electrolyser operation is switched off.
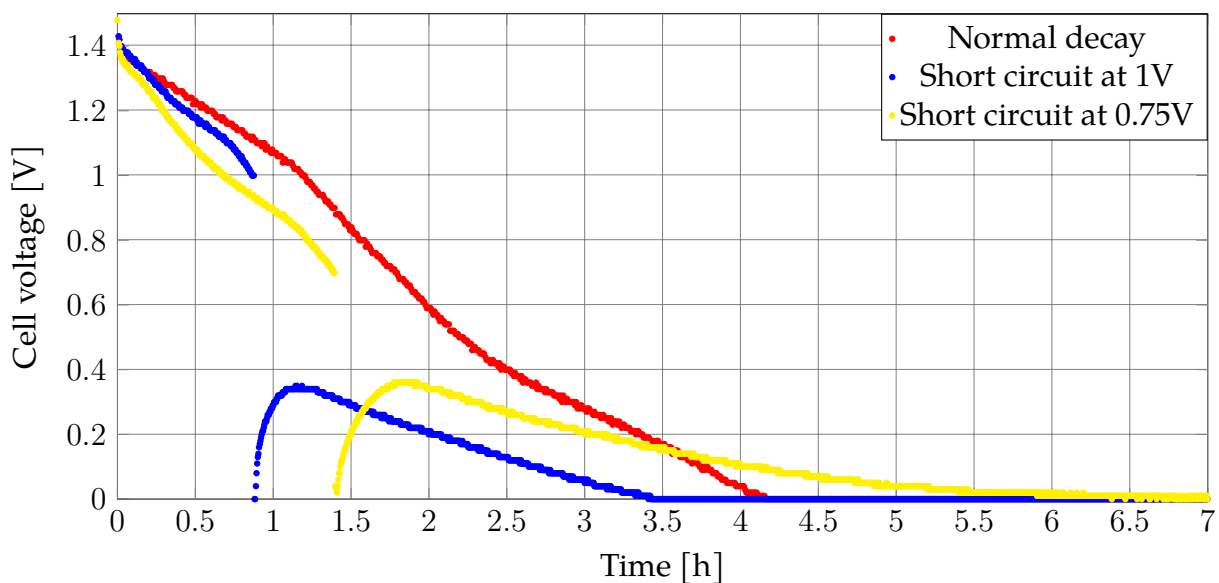
Figure 44: Voltage start-up at different current rates

5   Planning

The realization of this project include different topics and tasks. For this reason, it has been necessary to categorize the most important tasks, establish a road map for their completion and define deadlines in order to be able to complete the work before the deadline defined in the school regulations.

The followed planning can be seen in the figures 45,46 and 47 because for a better visualization in this document, the gantt chart is split in three consecutive periods. The main tasks that have been carried out in the work are presented as well as the waiting times caused by the purchase and shipping of components and the issues that have been necessary to solve.
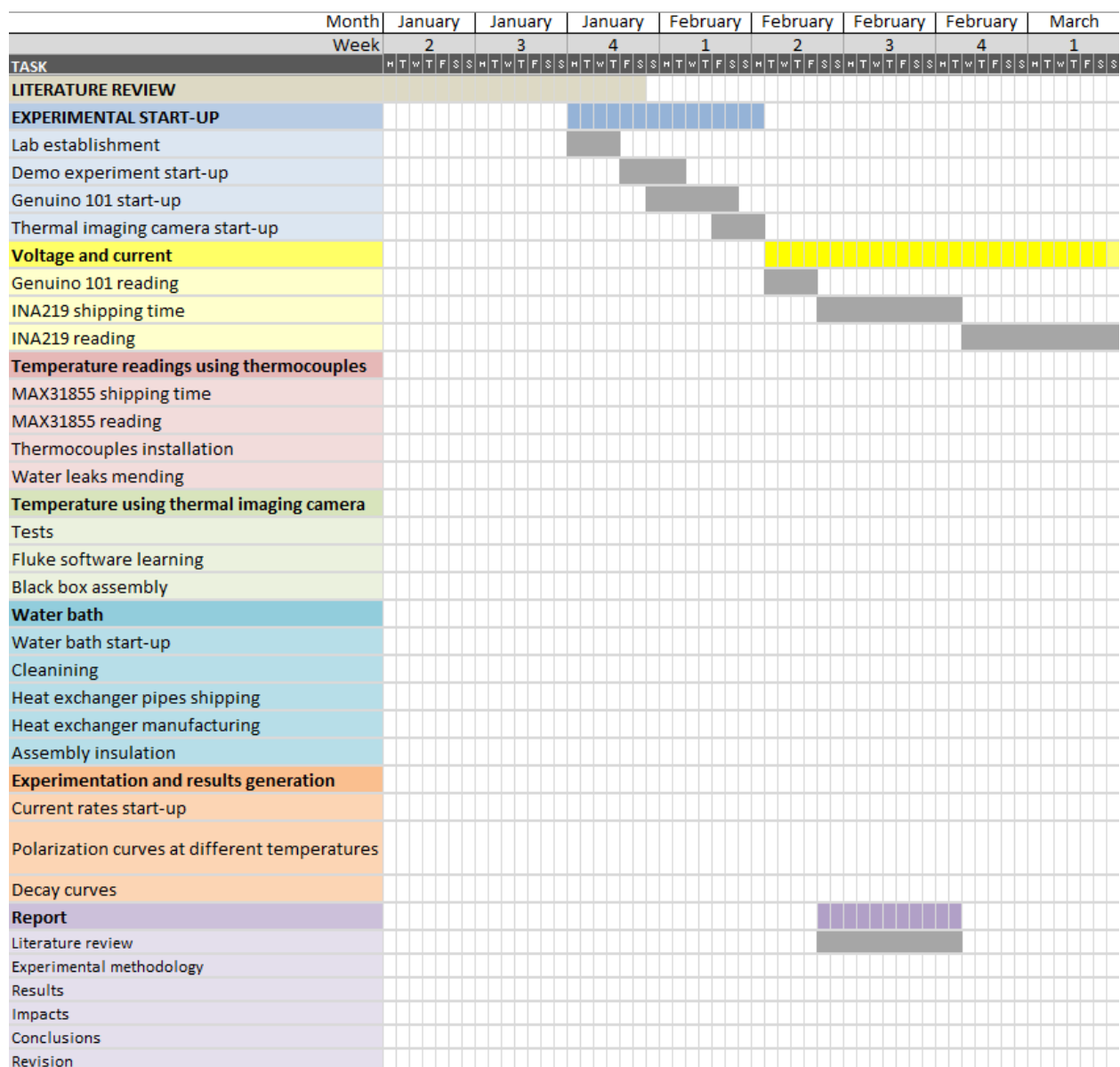
Figure 45: Gantt chart from 2nd week of January to 1st week of March

During the waiting times mainly caused by the shipping times of the INA219 and MAX31855, other tasks were performed as it can be observed in the gantt charts. During the INA219 shipping, the literature review part of the report was written. And while the MAX31855 was being shipped, the thermal camera readings were tested and the black box assembled.

Month	March	March	March	April	April	April	April	May
Week	2	3	4	1	2	3	4	1
TASK	HTWTFSS	HTWTFSS	HTWTFSS	HTWTFSS	HTWTFSS	HTWTFSS	HTWTFSS	HTWTFSS
LITERATURE REVIEW								
EXPERIMENTAL START-UP								
Lab establishment								
Demo experiment start-up								
Genuino 101 start-up								
Thermal imaging camera start-up								
Voltage and current								
Genuino 101 reading								
INA219 shipping time								
INA219 reading								
Temperature readings using thermocouples								
MAX31855 shipping time								
MAX31855 reading								
Thermocouples installation								
Water leaks mending								
Temperature using thermal imaging camera								
Tests								
Fluke software learning								
Black box assembly								
Water bath								
Water bath start-up								
Cleanining								
Heat exchanger pipes shipping								
Heat exchanger manufacturing								
Assembly insulation								
Experimentation and results generation								
Current rates start-up								
Polarization curves at different temperatures								
Decay curves								
Report								
Literature review								
Experimental methodology								
Results								
Impacts								
Conclusions								
Revision								

Figure 46: Gantt chart from 1st week of March to 1st week of May

ETSEIB

Figure 47: Gantt chart from 2nd week of May to 1st week of July

6 Environmental impact

Different resources have been used in this project, such as laboratory material, air conditioning elements and electronic components, among others. The calculation of the environmental impact generated due to the manufacture, operation and future disposal of all the different elements used would be too complex and sedulous work for the scope and purpose of this report. For this reason, it has been decided to calculate the environmental impact due to the operation of the elements used, quantifying the energy used and the carbon dioxide emissions generated caused by the energy consumption.
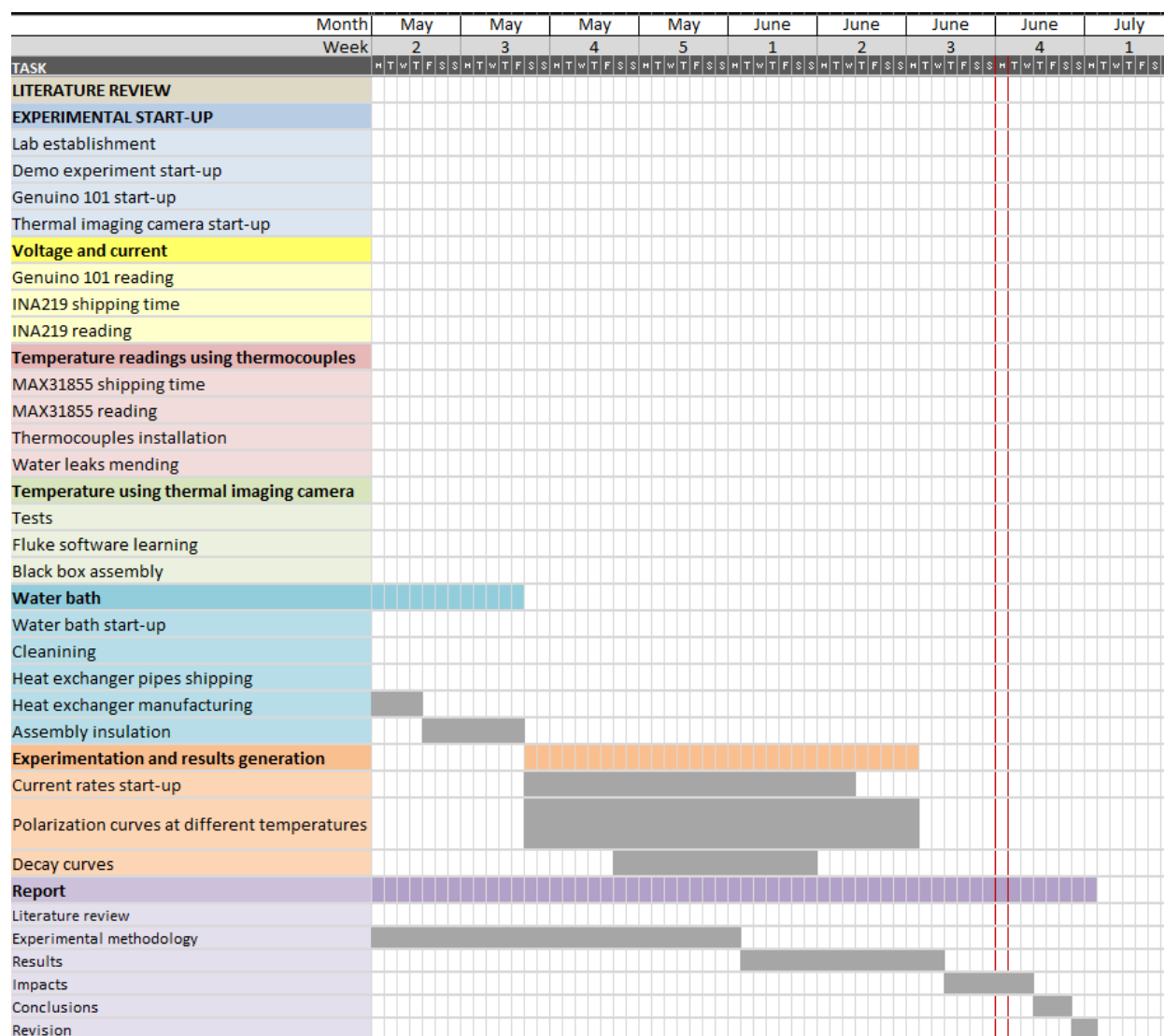
The air conditioning used in the workplaces used has been through an electric heater in the laboratory, without the possibility of cooling the place, and a heat pump in the office that allows heating and cooling depending on the needs. Causing that the energy source that is quantified throughout the environmental impact corresponds to electrical energy, since the rest of the devices also use electricity for their operation.

→ **Laboratory heating:** using an electric radiator of the brand Taurus has been used, which has a power of 2 [kW]. It has only been used during the winter months, for which 90 [hours] of use are estimated, producing an approximate electrical consumption of 180 [kWh].

→ **Office air conditioning:** a 1.5 [kWe] heat pump from Daikin brand has been used, which provides approximately 3.5 [kWt]. It is estimated that it has been used for 300 hours, but since it is controllable it has not been working at maximum power all the time and therefore it is assumed that the average power would have been 70% of the nominal power, giving rise to a total consumption of 315 [kWh].

→ **Lighting:** both in the laboratory and in the office there are LED lights which allow it to be kept illuminated. The estimated lighting power is 40 [W]. However, the number of hours used is estimated to be around 80 hours since most of the time the rooms have been illuminated by natural light. The lighting consumption is therefore estimated to be around 3.2[kWh].

→ **Computer and electronic devices:** the computer has been used not only to carry out the work, but also to power the Arduino 101, sensors, etc. An approximate consumption of 130 [W] and 600 hours is estimated, inducing to an approximate total consumption of 78 [kWh]. The thermal imaging camera is powered by a 75 [Wh] rechargeable battery, having required four full charges of the battery leading to a total consumption of 0.3 [kWh].

→ **Electrolyser power supply:** during the electrolyser operation, it is necessary to supply it with with an average a power of 2 [Wh]. A use of approximately 50 hours is estimated, generating a consumption of 0.1 [kWh].

→ **Water bath:** the nominal power of the water bath is 2 [kW] and it is estimated that its use has been about 20 hours, leading to a total consumption of 40 [kW].

The electricity consumed by other equipment used such as multimeter, calibration oven, or tin solder has been estimated at such small values that it is neglected in the

overall calculation.

All the electricity used is supplied from the Spanish national electrical grid, whose emissions and daily emission factor during the duration of the project can be seen in the following figure 48.
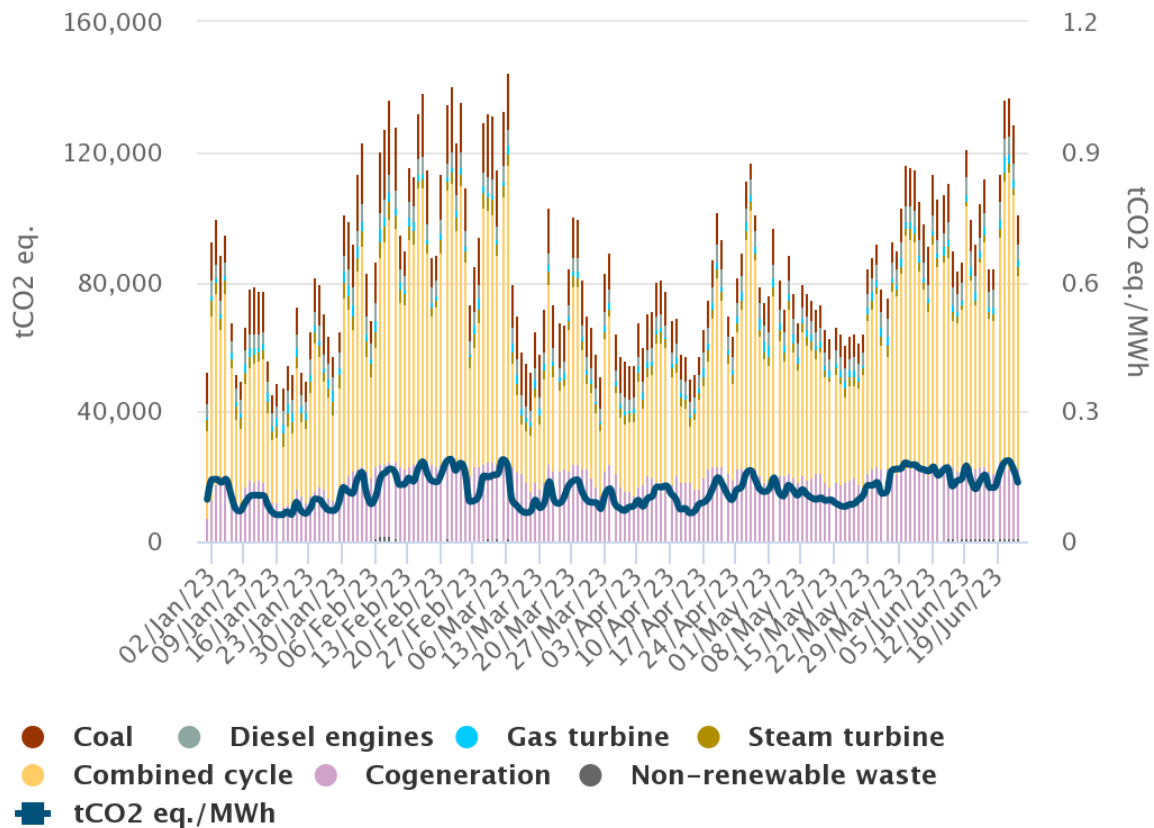
Figure 48: Spanish electrical grid emissions
Source: REE [19]

The average emission factor of the electrical system is 0.13 $[tCO_{2-eq}/MWh]$, giving rise to an environmental impact of the project of 80.16 $[tCO_{2-eq}/MWh]$. The following table 1 summarizes the consumption and the impact of each of the concepts included.

Concept	Consumption [kWh]	Environmental impact $[tCO_{2-eq}/MWh]$
Lab heating - electric heater	180	23.40
Air conditioning - Heat pump	315	40.95
Lightning	3.2	0.42
Computer	78	10.14
Thermal camera	0.3	0.04
Power Supply	0.1	0.01
Water bath	40	5.20
Total	616.6	80.16

Table 1: Environmental impact

7 Economical impact

In this section of the report, the costs associated with carrying out this work will be detailed, which are based on two main aspects: personnel costs and operating costs.

7.1 Personnel costs

Both the author, a graduate in industrial engineering, and the two advisors, engineers with more than 10 years of experience, have participated in this work. To define the corresponding hourly wages, the data published in the industrial sector section of the Adecco wage guide for the year 2022 [20] and for an annual working day of 1,826 hours has been taken as a reference. Obtaining that the salaries of the author and the tutors are 15 [€/hour] and 22.9 [€/hour] respectively. The following table 2 defines the hours worked by both to carry out this work and its associated cost.

Personnel	Working hours	Wage [€/hour]	Cost [€]
Authors	750	15	11,250
Advisors	100	22.9	2,290
Total personnel costs			13.666

Table 2: Personnel costs

7.2 Operational costs

The operational costs are those related to everything necessary to be able to carry out the work both in a practical way, both in its theoretical and practical part in the laboratory. These costs are listed below:

→ **Electricity:** corresponding to all the electricity used by the different equipment and that has already been previously calculated, showing the total calculated value of 616.6 [kWh] in the table 1.

Taking into account the average price of electricity in Spain for the year 2022, which is 0.3071 [€/kWh] [21], it can be established that the total cost of using equipment, air conditioning and lighting is 189.36 [€].

→ **Equipment depreciation:** the main assets used in the project that suffer depreciation are the computers, thermal bath, power supply, thermal camera, measurement equipment and the building itself in which the work has been carried out.

The computer used by the author corresponds to a Lenovo Legion Y520 model, which was purchased in 2017 at a cost of 1,000 [€] and is estimated to have a useful life of 8 years. As it is an electronic element, it has been decided to use the method of the sum of the digits of the years to calculate the annual depreciation suffered. This method is used to determine a higher depreciation in the first years of useful life and a lower depreciation at the end of the product life. The equation used to calculate its depreciation in its seventh year of useful life is the one defined in the equation 36, where the numerator is the useful life that the equipment still has, and

the denominator is the sum of the digits of all the years of useful life (being in this case: 1+2+3+4+5+6+7+8 = 36). Because the length of the project is 6 months and not a year, the depreciation cost of the computer is half of the one calculated, so a factor has been added to the end of the equation.

$$Computer\ depreciation\ rate\ [\%] = \frac{useful\ life \cdot 100}{sum\ of\ dígits}\frac{1}{2} = \frac{1 \cdot 100}{36}\frac{1}{2} = 2.\widehat{7}\,\% \qquad (36)$$

To calculate the workplace depreciation, it has been decided to use a linear depreciation method taking into account a useful life of 68 years, as indicated by the Spanish tax agency [22], leading to an annual depreciation rate of: 100 /68 = 1.47 [%]. To calculate the workplace cost, a room of 10 [m^2] has been taken in consideration with a cost of 3,776 [€/m^2] [23], taking the data for an apartment in Les Corts district in Barcelona because the author and the advisors carry out their work in this area. Also taking into account the already explained 6 months time span of the project, the depreciation cost of the building is that calculated in the equation 37.

$$Workplace\ depreciation\ cost\ [€] = 3.776 \cdot 10 \cdot 1,47\% \cdot \frac{1}{2} = 277.54\ [€] \qquad (37)$$

To calculate the costs associated with the use of the rest of the elements, it has been decided to take into account a linear depreciation over 20 years, resulting in an annual depreciation rate of 100/20 = 5%, so that the depreciation suffered during the project is 2.5% of the original purchase value.

$\rightarrow$ **Consumable material:** throughout the project it has been necessary to use different materials that have been completely consumed and therefore their full cost must be taken into account.

The following table 3 shows the operation costs of all the equipment used in the project.

ETSEIB

Concept		Use	Unitary cost	Cost [€]
Electricity		616.6 [kWh]	0,3071 [€/kWh]	189.34 [€]
Assets depreciation	Computer	6 months	1.000 [€/ud]	27.77
	Workplace	10 m^2	3.776 [€/m^2]	277.54
	Electrolyser	6 months	260 [€/ud]	6.50
	4 MAX31855	6 months	3.98 [€/ud]	0.40
	Calibration oven	6 months	150 [€/ud]	3.75
	INA219	6 months	9.79 [€/ud]	0.25
	Power Supply	6 months	605 [€/ud]	15.13
	Multimeter	6 months	130 [€/ud]	3.25
	Water bath	6 months	250 [€/ud]	6.25
	Tin solder	6 months	45 [€/ud]	1.13
	Thermal camera	6 months	15,500 [€/ud]	387.50
	Arduino 101	6 months	25 [€/ud]	0.63
	Connection cables	6 months	10 [€/ud]	0.25
Consumable material	Tape	-	9 [€/ud]	9.00
	Distilled water	5 liters	3 [€/l]	15.00
	Sealant	-	4 [€/ud]	4.00
	3D printed parts	-	0.35 [€/g]	15.62
	Cooper tubes	-	14.26 [€/ud]	14.26
	Insulation foam	1 [m^2]	3 [€/m^2]	3.00
Total operational cost				980.57 [€]

Table 3: Operational costs

Finally, the total costs of the project amount to 14,646.57 [€], corresponding to the sum of all personnel and operational costs.

8 Social and gender impact

The use of hydrogen as an alternative technology to the use of fossil fuels has a significant impact on different social aspects, such as health and fair access to energy.

Regarding the impact on health, the reduction of fossil fuels mainly allows the improvement of air quality. The burning of fossil fuels, such as coal, oil, and natural gas, is one of the main sources of air pollution. These fuels emit a variety of pollutants, including fine particles (PM2.5), sulfur dioxide (SO_2), nitrogen oxides (NO_x), and volatile organic compounds (VOCs), among others. These contaminants can enter in the lungs and cause respiratory problems such as asthma, bronchitis, emphysema, and other respiratory infections. Chronic exposure to air pollution has also been associated with increased risk of cardiovascular diseases, such as heart disease, stroke, high blood pressure, and arrhythmias. Some pollutants emitted from the burning of fossil fuels, such as volatile organic compounds (VOCs) and products of incomplete combustion, have been linked to an increased risk of cancer, including lung and bladder cancer. Finally, fossil fuels reduction would also allow for mental health benefits since long-term exposure to air pollution has been associated to an increased risk of mental health problems, such as stress, depression and anxiety. Ultimately, the use of hydrogen would allow the reduction of the use of fossil fuels, improving air quality and the health of the population, mitigating the appearance of pulmonary, cardiovascular, cancer and psychological diseases [24] [25] [26].

The use of hydrogen as an energy source can have a positive impact from a justice and social equity perspective. To achieve this, it is important to ensure that marginalized communities, who often have limited access to modern and reliable energy services, can also be benefited from hydrogen-based solutions, aided by electricity generation from renewable sources, which allow electricity generation emission-free in remote locations. This can be achieved through the implementation of policies and programs that prioritize the supply of clean energy to these communities while ensuring that the costs are affordable. However, the transition to hydrogen must include training programs for the local communities personnel in charge of the necessary infrastructure.

Although the hydrogen industry is still in its early stages, there are already jobs related to hydrogen production, distribution and storing. Currently, there is a gender gap in the participation of women in STEM (science, technology, engineering, and mathematics) fields, which could translate into a lower representation of women in these emerging jobs. Specifically in Spain, despite there are the same access opportunities for training in any field, in 2022, 25% of graduates in STEM careers are women. It is also important to ensure equal participation of women in decision-making processes. However, in many cases, women are underrepresented in leadership spaces and in decision-making roles in energy and technology sectors, since 25% of managerial positions in companies are held by women [27] [28].

In the elaboration of this work a feminist criteria has been followed; maintaining at all times equal rights between men and women. In addition, the guidelines established in the gender equality resources framed within the 2022-2026 equality plan of the university has been followed [29].

ETSEIB

Conclusions

In the first part of this work, it has been possible to monitor the supply voltage and current variables to the electrolyser in a very precise way. This has allowed to obtain the polarization curves not only in steady state but also to show the behavior and dependence of the polarization voltage as a function of the current rate applied during the start-up of the electrolyser. Thanks to doing it digitally, it has been possible to use high sampling rates (up to 10 data per second) and also allow data collection automatically for several hours. As a result, it has been seen that the electrolyser takes a long time to depolarize once turned off, and that even when making a short circuit between its terminals, the electrolyser recovers part of the voltage it previously had.

These start-up and decay behaviors of the electrolyser may be relevant depending on the application for which it is intended. And perhaps these results are an aspect to take into account in the operation of the electrolysers depending on the characteristics of the application.

From a thermodynamic point of view, the objective of having polarization curves at different temperatures has been fulfilled, having verified that the higher the operating temperature, the higher the operating voltage at the same current density.

However, the monitoring of hydrogen production has not been satisfactory, giving results inconsistent and without any relation to the operating temperature, since the calculated Faraday efficiency does not have logical values. For this reason, it has not been possible to clarify whether the operation of the electrolyser at a higher temperature, which entails a greater electrical consumption, is equivalent to a greater or lesser hydrogen production.

Although the data collection of current and voltage has been carried out accurately and with high resolution, this has not been the case for the measurement of temperatures and hydrogen production. Therefore, the use of thermocouples, voltage risers and ADC that achieve a better resolution than the one used in this project ($\pm$ 0.25°C) is recommended for future work. The use of higher inlet flow rates to the electrolyser is also proposed to achieve good oxygen drag, which could be controlled since the higher the current density supplied to the electrolyser, the greater the dissociation of water and therefore the greater the need for oxygen drag. The design of a reliable, accurate and leak-free hydrogen production measurement system will be important. Finally, it is suggested to change the methacrylate plates of the electrolyser, sifting to a material that is transparent to the short and long wave infrared spectrum. This could allow the visualization using the available thermal camera of the temperature gradient caused by the electrochemical reaction without having an intermediate material that distorts these measurements.

In spite of the suggested future works, for the realization of most of these suggestions it is necessary to disassemble and modify the electrolyser used -being able to spoil it in the process-, or the use of another type of electrolyser assembly with a design thought for needs of the project.

References

[1] NASA Earth Science Communications Team. 'Climate change VS global warming'. Available at: `https://climate.nasa.gov/global-warming-vs-climate-change/` (Accessed: 2023-1-10).

[2] Met Office College. 'Causes of climate change'. Available at: `https://www.metoffice.gov.uk/weather/climate-change/causes-of-climate-change` (Accessed: 2023-1-10).

[3] Center for climate and energy solutions. 'Gloabl emissions'. Available at: `https://www.c2es.org/content/international-emissions/` (Accessed: 2023-1-10).

[4] McKinsey & Company. 'The net-zero challenge: Accelerating decarbonization worldwide '. Available at: `https://www.mckinsey.com/capabilities/sustainability/our-insights/the-net-zero-challenge-accelerating-decarbonization-worldwide` (Accessed: 2023-1-12).

[5] Eric Koons. 'The Pros and Cons of Hydrogen Energy'. *Energy Tracker Asia*. Available at: `https://energytracker.asia/pros-and-cons-of-hydrogen-energy/` (Accessed: 2023-2-15).

[6] Office of energy efficiency and renewable energy. 'Hydrogen production processes'. Available at: `https://www.energy.gov/eere/fuelcells/hydrogen-production-processes` (Accessed: 2023-3-17).

[7] Jhonson Matthey. 'Steam reforming catalysts'. Available at: `https://matthey.com/products-and-markets/chemicals/steam-methane-reforming` (Accessed: 2023-1-17).

[8] Industrial Scientific. 'Carbon Monoxide vs. Carbon Dioxide: Let's Compare'. Available at: `https://www.indsci.com/en/blog/carbon-monoxide-vs.-carbon-dioxide-lets-compare` (Accessed: 2023-1-17).

[9] Pierre Millet and Sergey Grigoriev. 'Renewable Hydrogen Technologies', *Elsevier Science*, chapter 2 pp. 19-40, 2013. [Online]. Available at: `http://dx.doi.org/10.1016/B978-0-444-56352-1.00001-5`. Accessed: 2023-1-27.

[10] Luis M. Gandía and Gurutze Arzamendi and Pedro M. Diéguez. 'Renewable Hydrogen Technologies. Production, Purification, Storage, Applications and Safety' in *Renewable Hydrogen Technologies*, Pamplona, Spain: *Elsevier Science*, chapter 2.2 pp. 25-29, 2013. [Online]. Accessed: 2023-1-27.

[11] Luis M. Gandía and Gurutze Arzamendi and Pedro M. Diéguez. 'Renewable Hydrogen Technologies. Production, Purification, Storage, Applications and Safety' in *Renewable Hydrogen Technologies*, Pamplona, Spain: *Elsevier Science*, chapter 2.3 pp. 29-36, 2013. [Online]. Accessed: 2023-1-27.

[12] Luis M. Gandía and Gurutze Arzamendi and Pedro M. Diéguez. 'Renewable Hydrogen Technologies. Production, Purification, Storage, Applications and Safety' in *Renewable Hydrogen Technologies*, Pamplona, Spain: *Elsevier Science*, chapter 2.4 pp. 36-39, 2013. [Online]. Accessed: 2023-1-27.

[13] Vicenzo L. et al. 'Modelling and Experimental Analysis of a Polymer Electrolyte Membrane Water Electrolysis Cell at Different Operating Temperatures ', *Energies*, vol. 11, n.º 12, nov 2018 [Online]. Available at: `https://doi.org/10.3390/en11123273`. Accessed: 2023-1-20.

[14] HardKernel. 'Odroid XU-4'. Available at: `https://www.hardkernel.com/shop/odroid-xu4-special-price/` (Accessed: 2023-2-5).

[15] Raspberry Pi. 'Raspberry Pi 3 Model B+'. Available at: `https://www.raspberrypi.com/products/raspberry-pi-3-model-b-plus/` (Accessed: 2023-2-5).

[16] Arduino. 'Arduino 101'. Available at: `https://docs.arduino.cc/retired/boards/arduino-101-619` (Accessed: 2023-2-5).

[17] Phywe. 'Main page website'. Available at: `https://www.phywe.com/` (Accessed: 2023-2-10).

[18] Adafruit. 'Arduino libraries'. Available at: `https://learn.adafruit.com/adafruit-all-about-arduino-libraries-install-use/arduino-libraries` (Accessed: 2023-2-26).

[19] Red Eléctrica España. 'CO2 EQ. emission factor and GHG emissions regarding non-renewable generation'. Available at: `https://www.ree.es/en/datos/generation/non-renewable-detail-CO2-emissions` (Accessed: 2023-5-29).

[20] Adecco Industrial, 'Sector Industrial', en *Guía salarial 2022*. Adecco, España, Guía, 2022.[Online]. Available at: `https://www.adecco.es/guia-salarial`. Acceso: 2 de marzo de 2023.

[21] Datosmacro. 'España - Precios de la electricidad en los hogares'. Expansión/Datosmacro. `https://datosmacro.expansion.com/energia-y-medio-ambiente/electricidad-precio-hogares/espana` (Accessed: 2023-6-5).

[22] Agencia Tributaria. *Manual de actividades económicas. Obligaciones fiscales de empresarios y profesionales residentes en territorio español*. España. 2023. [En línea] Disponible en: `https://sede.agenciatributaria.gob.es/Sede/ayuda/manuales-videos-folletos/manuales-practicos/folleto-actividades-economicas/3-impuesto-sobre-renta-personas-fisicas/3_5-estimacion-directa-simplificada/3_5_4-tabla-amortizacion-simplificada.html`

[23] RealAdvisor. 'Precio de la vivienda'. `https://realadvisor.es/es/precios-viviendas/08028-barcelona` (acceso: 10 de marzo de 2023).

[24] Jerrett, M. et al. 'Spatial analysis of air pollution and mortality in California'. *American Journal of Respiratory and Critical Care Medicine*, April 2014. [Online]. Available at: `https://doi.org/10.1164/rccm.201303-0609OC`. Accessed: 2023-6-10.

[25] Brook, R.D. et al. 'Particulate matter air pollution and cardiovascular disease'. *American Heart Association*, May 2010. [Online]. Available at: `https://www.ahajournals.org/doi/10.1161/CIR.0b013e3181dbece1`. Accessed: 2023-6-10.

[26] World Health Organization.' Review of evidence on health aspects of air pollution - REVIHAAP Project: Final Technical Report'. Available at: `https://apps.who.int/iris/handle/10665/341712` (Accessed: 2023-6-10).

[27] European Union Statistical Office. 'Statistical Themes - Equality'. Available at: `https://ec.europa.eu/eurostat/web/equality` (Accessed: 2023-6-10).

[28] Organization for Economic Cooperation and Development (OECD). 'Gender equality and work'. Available at: `https://www.oecd.org/stories/gender/gender-equality-and-work` (Accessed: 2023-6-10).

[29] Universidad Politécnica de Cataluña. "Igualtat de gènere a la UPC". Pla d'igualtat - Recursos. Available at: `https://igualtat.upc.edu/ca/recursos` (Accessed: 2023-6-20).